



# Upcycled C&D waste as recycled concrete aggregate for green cementitious composites: Mechanical, NDT and post-fire performance

Nisar Ali Khan<sup>a</sup>, Angelo Aloisio<sup>b,\*</sup>, Rafia Younas<sup>c</sup>, Flavio Stochino<sup>d</sup>, Giorgio Monti<sup>e</sup>

<sup>a</sup> Department of Civil Engineering, Faculty of Engineering & Technology, International Islamic University, Sector H-10, Islamabad 44000, Pakistan

<sup>b</sup> Department of Civil, Construction-Architectural and Environmental Engineering, Università degli Studi dell'Aquila, L'Aquila, 67100, Italy

<sup>c</sup> Department of Environmental Sciences, Faculty of Agriculture, Gomal University, Dera Ismail Khan, Pakistan

<sup>d</sup> Department of Civil Environmental Engineering and Architecture, University of Cagliari, 09123 Cagliari, Italy

<sup>e</sup> Department of Civil Engineering, Xi'an JiaoTong-Liverpool University, 111 Ren'ai Road, Suzhou 215123, China

## ARTICLE INFO

### Keywords:

Recycling  
Construction materials  
Sustainability  
Innovation  
Infrastructure development  
Waste management  
Green practices  
Economic viability

## ABSTRACT

Although recycled aggregate concrete (RAC) has been widely investigated, its performance remains strongly dependent on the origin, quality, and processing history of the recycled aggregate. This study addresses this issue through a context-specific experimental assessment of recycled coarse aggregates (RCA) produced from locally sourced construction and demolition (C&D) concrete waste in Pakistan, where natural aggregate extraction is increasingly constrained and systematic RCA data remain limited. Unlike many previous studies based on generic or laboratory-produced recycled aggregates, the RCA used here was obtained from demolished rigid pavement concrete along the Old Grand Trunk (GT) Road corridor, providing a traceable and representative waste stream for local infrastructure applications.

Natural coarse aggregates were replaced by RCA at 0%, 25%, 50%, 75%, and 100% by mass. The experimental programme combined aggregate characterization, destructive mechanical testing, non-destructive evaluation, post-fire residual strength assessment after exposure to 500 °C, and microstructural/mineralogical analyses using SEM, EDS, and XRD. RCA exhibited higher water absorption and lower specific gravity than natural aggregates because of adhered mortar, microcracking, and increased porosity. Mechanical results showed a gradual reduction in compressive, flexural, and tensile strength with increasing RCA content; however, mixtures containing up to 50% RCA achieved 28-day compressive strengths suitable for structural-grade concrete. One-way ANOVA indicated that the differences among replacement levels were not statistically significant at the 95% confidence level under the investigated conditions.

The microstructural observations confirmed that RCA incorporation mainly affects concrete through increased porosity and thickening of the interfacial transition zone, while the fundamental hydration products remain comparable to those of conventional concrete. The results demonstrate that locally sourced Pakistani RCA can be incorporated in structural concrete, particularly up to 50% replacement, with acceptable mechanical performance. The study therefore contributes region-specific evidence for sustainable aggregate substitution, C&D waste valorisation, and circular construction practices in Pakistan.

## 1. Introduction

Construction and demolition (C&D) activities generate substantial quantities of waste during the construction, renovation, retrofitting, and demolition of infrastructure. Globally, billions of tons of C&D waste are produced each year, placing increasing pressure on natural resources and waste management systems [1]. Beyond the environmental burden, C&D waste also represents a technically heterogeneous secondary

resource whose engineering value depends on its source, composition, contamination level, crushing procedure, and degree of residual mortar attachment. Therefore, the challenge is not only to divert waste from landfills, but also to transform highly variable demolished materials into reliable constituents for structural concrete. In many countries, the lack of adequate processing and recycling facilities results in most C&D waste being disposed of in landfills rather than being reused in new

\* Corresponding author.

Email addresses: [nisar.ali@iiu.edu.pk](mailto:nisar.ali@iiu.edu.pk) (N. Ali Khan), [angelo.aloisio1@univaq.it](mailto:angelo.aloisio1@univaq.it) (A. Aloisio), [dr.rafia@gu.edu.pk](mailto:dr.rafia@gu.edu.pk) (R. Younas), [fstochino@unica.it](mailto:fstochino@unica.it) (F. Stochino), [giorgio.monti@uniroma1.it](mailto:giorgio.monti@uniroma1.it) (G. Monti).

<https://doi.org/10.1016/j.istruc.2026.112330>

Received 18 February 2026; Received in revised form 15 May 2026; Accepted 8 June 2026

2352-0124/© 2026 The Author(s). Published by Elsevier Ltd on behalf of Institution of Structural Engineers. This is an open access article under the CC BY license (<http://creativecommons.org/licenses/by/4.0/>).

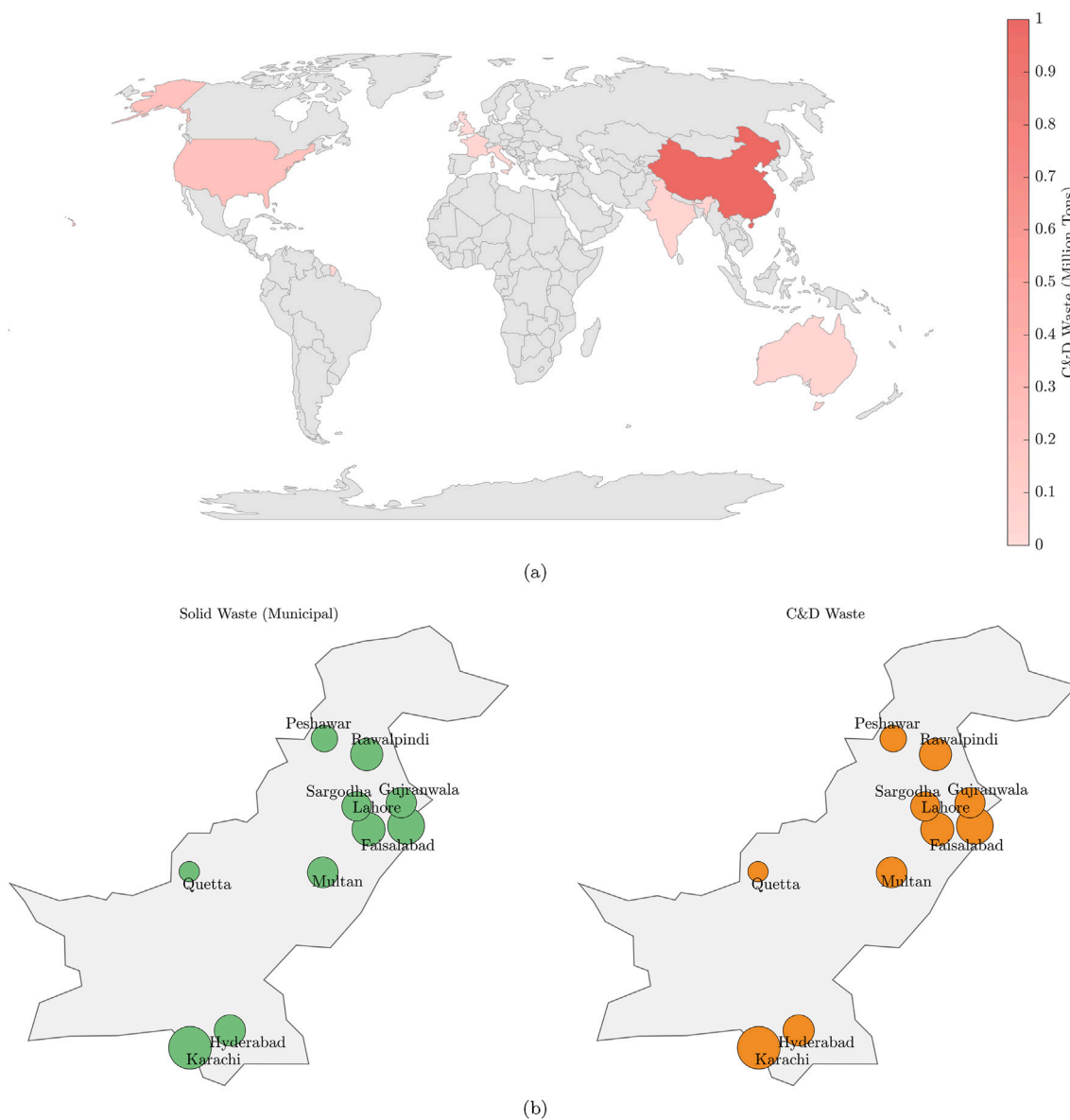


**Fig. 1.** (a) Global distribution of construction and demolition (C&D) waste generation for selected countries, see Table 1. (b) Global distribution of C&D waste generation for Pakistan adapted from [5].

construction. Consequently, only a small fraction of this waste stream is currently recycled or used as a substitute for naturally sourced aggregates.

The reuse of C&D materials as a replacement for natural aggregates has therefore become a key priority within the circular economy framework. Each year, approximately 20 billion tons of natural resources are consumed for concrete production, and this demand is expected to triple within the next two to three decades. At the same time, the demolition of existing structures contributes significantly to global solid waste generation, accounting for 20–40% of the total waste stream and posing severe environmental challenges [2]. Although recycling rates vary across regions, notable disparities exist: for instance, the United States recycles nearly 75% of its 600 million tons of annual C&D waste, whereas China recycles less than 40%, and India recovers and recycles only about 1% [3]. These trends highlight the urgent need for effective C&D waste management practices worldwide [4], see Fig. 1(a) and Table 1. However, high recycling rates alone do not necessarily guarantee high-value reuse. In many cases, recycled materials are still downcycled into low-grade

applications such as road sub-base layers, backfilling, or temporary works. A more demanding and scientifically relevant objective is the structural reuse of recycled concrete aggregate (RCA) in new cementitious composites, where mechanical reliability, durability, and quality control requirements are considerably stricter.

Similar challenges are observed in Europe, where C&D waste represents nearly 30% of total waste generation (Eurostat, 2020). Improper handling of C&D waste can lead to soil and water contamination, public health risks, and economic burdens associated with landfill expansion [17]. Recycling and reusing C&D waste have been identified as effective strategies for mitigating these impacts, offering benefits such as conserving natural aggregates, reducing landfill volume, and lowering greenhouse gas emissions [18,19]. Among these materials, concrete is of particular interest: recycled concrete aggregate (RCA) can partially or fully replace natural aggregate in new concrete production, often yielding comparable mechanical performance [20]. However, widespread adoption is hindered by the variability of RCA properties, lack of standardization, and additional processing costs [21]. This variability is a

central scientific issue in recycled aggregate concrete (RAC). Unlike natural aggregates, RCA is a composite material consisting of original natural stone, adhered old mortar, microcracks generated during demolition and crushing, and pre-existing interfacial transition zones. As a result, RCA affects concrete not only through aggregate replacement, but also through changes in water demand, packing density, pore connectivity, internal curing, and the formation of new and old ITZ systems. Continued research is therefore essential to establish reliable guidelines and improve the performance of RCA-based concrete mixtures.

Extensive research has documented that RCA generally leads to reductions in mechanical performance, typically 5–30% lower compressive strength at full replacement levels, primarily due to the presence of residual mortar and weakened interfacial transition zones (ITZ) [22–26]. Nonetheless, when replacement is limited to 20–30%, strength losses are often negligible [24,27]. Tensile and flexural strengths follow a similar trend, with reductions typically under 15% [28,29]. Elastic modulus is consistently lower by 20–30% [29,30], and fatigue performance is also adversely affected at high RCA content [31,32]. Despite these limitations, high-performance RCA with compressive strengths exceeding 50 MPa is achievable through mix optimization and mineral admixtures [33–36]. These findings indicate that the influence of RCA is not governed solely by the replacement ratio. Instead, it is controlled by a coupled set of parameters, including parent concrete strength, adhered mortar volume, crushing intensity, moisture conditioning, aggregate grading, and the compatibility between the recycled aggregate surface and the new cement paste. Consequently, replacement percentage should be interpreted together with RCA quality and processing history. This explains why apparently similar RAC mixtures may show different mechanical responses across studies.

Durability remains a critical concern. RCA's higher porosity increases water absorption, chloride permeability, carbonation depth, and shrinkage strains [30,35,37–40]. Measures such as lowering the water/cement ratio, using supplementary cementitious materials, or pre-treating RCA have been shown to mitigate these effects [28,35,41]. Microstructural studies confirm that RAC has higher void content and more pronounced ITZs, yet treatments like carbonation and nano-silica coatings can improve ITZ quality and reduce microcracking [32,42–45]. From a microstructural perspective, RAC differs from conventional concrete because it may contain at least two generations of ITZ: the old ITZ inherited from the parent concrete and the new ITZ formed between RCA and fresh cement paste. These overlapping weak zones can promote crack initiation, while the porous adhered mortar can act either as a defect or as an internal curing reservoir depending on its saturation state and the mixture design. This dual role explains the non-monotonic trends sometimes reported in mechanical and durability properties at intermediate RCA contents.

Another aspect requiring deeper investigation is the residual performance of RAC under extreme actions, particularly elevated temperatures. Fire exposure may dehydrate cement hydrates, increase pore pressure, weaken aggregate–paste bonding, and intensify microcracking. In RCA concrete, these mechanisms may be amplified by the presence of old mortar and pre-existing cracks, but internal porosity may also relieve thermal stresses and reduce explosive damage. Therefore, post-fire behaviour cannot be inferred directly from ambient-temperature strength results. A combined assessment based on mechanical tests, non-destructive evaluation, and microstructural observations is needed to clarify how RCA modifies the damage mechanisms after thermal exposure.

Recent studies have increasingly focused on improving RCA quality through surface modification and treatment techniques rather than simply limiting the replacement ratio. These approaches include cement-paste or cement-slurry coating, chemical treatment, abrasion treatment, and combined treatment procedures aimed at removing or densifying adhered old mortar and improving the RCA–paste bond. Panghal and Kumar [46] showed that surface modification of recycled coarse aggregates can improve the mechanical response of RCA concrete by

**Table 1**  
Annual construction and demolition (C&D) waste generation by country or region.

Country / Region	Annual C&D Waste	Remarks	Reference
China	2300 million tonnes	Largest global C&D waste producer due to rapid urbanization	[6]
European Union (EU-27)	850 million tonnes	High generation, varied recycling rates across member states	[7]
United States	700 million tonnes	Major contribution with significant recovery infrastructure	[8]
India	350–750 million tonnes	Rapid urban development; low recycling infrastructure	[9]
Brazil	100 million tonnes	Significant South American contributor	[10]
Japan	85 million tonnes	Moderate waste generation with advanced recycling	[11]
South Korea	62 million tonnes	Substantial waste with stronger recycling systems	[12]
United Kingdom	70 million tonnes	Historic estimates of national C&D generation	[13]
Australia	20–40 million tonnes	Smaller total but rising generation trend	[14]
Canada	30–35 million tonnes	Moderate generation relative to US	[15]
Pakistan	12–16 million tonnes	Smaller total but rising generation trend	[16]

enhancing the quality of the interfacial transition zone. In a subsequent study, abrasion combined with cement-slurry treatment was reported to improve concrete durability and strength by reducing the negative influence of weak residual mortar [47]. Similarly, the comparative assessment of coating, chemical, and abrasion treatments demonstrated that chemical and cement-slurry treatments can significantly improve compressive, flexural, and splitting tensile performance, with SEM and XRD evidence indicating a denser microstructure and improved aggregate–paste interaction [48]. These studies highlight that the performance of RAC depends not only on the replacement percentage, but also on RCA surface condition, ITZ quality, and the effectiveness of pre-treatment methods.

On the sustainability front, RCA offers substantial environmental benefits by reducing the burden on landfills and raw material consumption. Life-cycle assessments (LCAs) indicate that RCA can reduce the global warming potential of concrete by 5–15%, depending on mix design and transport logistics [49–51]. In practice, standards such as EN 206 and BS 8500 permit limited RCA use in structural applications, with stricter limits for higher strength classes. However, code acceptance varies globally, with progressive adoption in Europe and Asia, and limited implementation in South America and parts of South Asia [24,52,53]. This uneven regulatory acceptance reflects the fact that sustainability benefits must be balanced against uncertainty in engineering performance. For structural applications, the key question is not whether RCA can reduce environmental impact, but under which replacement levels, exposure conditions, and quality-control procedures it can do so without compromising safety, serviceability, and durability.

Despite the growing literature, significant research gaps persist. These include limited data on RCA's long-term behavior (e.g., fatigue, fire, seismic performance), lack of large-scale field validations, and underrepresentation of geographic regions such as South Asia, Africa, and the Middle East [54–56]. Particularly in Pakistan, where construction waste is abundant, comprehensive studies are scarce. This regional gap is important because RCA performance is strongly site-specific.

Parent concrete composition, demolition practices, crushing procedures, environmental exposure history, and local aggregate mineralogy differ substantially from one country to another. Therefore, experimental evidence obtained in regions with mature recycling systems cannot be directly transferred to Pakistan, where RCA production is still emerging and where construction practices, aggregate sources, and waste-management infrastructure are different.

In Pakistan, see Fig. 1(b), C&D waste management is closely connected to both environmental pressures and current economic constraints affecting the construction sector. C&D activities are estimated to account for approximately 30% of the country's total solid waste, while in Punjab material wastage at construction sites represents about 9.8% of regional waste generation. Considering that Pakistan produces approximately 48.5 million tons of solid waste annually, the C&D fraction may contribute nearly 14 million tons per year. Major urban centres are the main contributors to this waste stream; for example, Karachi alone generates more than 13,500 tons of municipal waste per day. These figures indicate that C&D waste is not a marginal by-product, but a substantial and growing material flow that requires systematic recovery and reuse strategies.

At the same time, Pakistan faces increasing pressure on the supply of natural aggregates. Recent restrictions on quarrying activities in the Margalla Hills, one of the main sources of natural aggregates for construction, have intensified supply-chain difficulties, increased material costs, and contributed to project delays. This situation is further aggravated by rapid urbanization, population growth, and the expansion of transport and building infrastructure, all of which are expected to increase the national demand for construction aggregates. Therefore, Pakistan must diversify its aggregate sources and reduce its dependence on natural quarry materials.

The adoption of recycled C&D materials, and particularly recycled concrete aggregate (RCA), represents a technically and environmentally relevant strategy in this context. RCA use can reduce landfill disposal, conserve natural aggregate resources, lower transportation and material costs, and support circular construction practices within the national construction sector. Among the possible C&D waste streams, pavement-derived concrete waste is particularly significant for Pakistan because road rehabilitation and reconstruction projects generate large volumes of relatively homogeneous demolished concrete. Compared with mixed building demolition debris, pavement concrete is often more traceable in terms of original material composition, strength class, and service conditions. If properly processed, graded, and characterized, this waste stream can provide RCA with more predictable engineering properties, thereby improving the feasibility of its use in structural concrete applications.

This study addresses the limited availability of experimental data on concrete incorporating RCA derived from locally sourced C&D waste in Pakistan. Although RCA has been extensively investigated in other regions, the direct transfer of existing findings to the Pakistani construction sector remains uncertain because RCA performance is strongly influenced by parent concrete quality, aggregate mineralogy, demolition practices, crushing procedures, adhered mortar content, and local mix-design conventions.

The novelty of the present work is therefore not related to the use of unconventional test methods, but to the source-specific and region-specific validation of RCA obtained from an actual infrastructure waste stream in Pakistan. In particular, the recycled aggregate was produced from demolished rigid pavement concrete collected along the Old Grand Trunk Road corridor, providing a traceable and locally representative material source rather than a generic or laboratory-produced RCA. This is relevant because pavement-derived concrete waste is generally more homogeneous than mixed demolition debris and may represent a practical route for converting road-rehabilitation waste into structural concrete constituents.

To respond to this gap, the present work evaluates concrete mixtures incorporating 0%, 25%, 50%, 75%, and 100% RCA replacement under standardized testing conditions. The experimental programme

integrates aggregate characterization, compressive, flexural, and split tensile testing, rebound hammer and ultrasonic pulse velocity measurements, water absorption tests, residual mechanical assessment after exposure to 500 °C, and SEM-EDS-XRD analyses. The contribution of the study lies in this integrated multi-scale interpretation, which links the mechanical and non-destructive responses of RCA concrete to pore structure, ITZ quality, mineralogical composition, and thermally induced damage mechanisms.

Accordingly, the study provides context-specific evidence for the structural use of Pakistani pavement-derived RCA and identifies replacement levels that offer a practical compromise between sustainability benefits and mechanical reliability. The results are intended to support the informed valorisation of C&D concrete waste in Pakistan, where natural aggregate extraction is increasingly constrained and systematic RCA quality-control data remain limited.

## 2. Materials and methods

This study investigates the mechanical and durability performance of concrete incorporating RCA derived from C&D waste. The experimental programme was designed to evaluate the feasibility of partially or fully replacing natural coarse aggregates with RCA in structural concrete. The methodology includes aggregate characterisation, concrete mix design, specimen casting and curing, and a combination of destructive and non-destructive testing procedures.

### 2.1. Case study and source of recycled aggregates

The C&D waste used in this study was sourced from the Old Grand Trunk Road (GT Road), a central transportation corridor in Pakistan. The selected road section extends from Faizabad to Rawat, where rehabilitation and reconstruction activities necessitated the removal of the existing rigid pavement structure. The road was selected as a case study because of the availability of well-documented construction records and the known engineering properties of the original pavement materials. The removed pavement primarily consisted of plain cement concrete, typical of rigid road pavements designed to sustain heavy traffic loads and long service life. Based on available construction records and standard highway engineering practice, the original pavement concrete was produced using natural coarse aggregates, natural fine aggregates, and ordinary Portland cement, and can be classified as normal-weight structural concrete of strength class C35/45. The pavement was constructed in accordance with the prevailing national highway specifications and internationally recognised standards applicable at the time of execution, consistent with conventional rigid pavement design requirements.

The pavement removal was carried out under the supervision of the Frontier Works Organisation (FWO), ensuring a reliable and traceable source of concrete with known engineering properties. Large chunks of demolished pavement were manually reduced using jackhammers and sledgehammers, after which the material was mechanically crushed into smaller fractions suitable for reuse, as shown in Fig. 2. The crushed debris was sieved according to ASTM specifications to obtain the required particle-size categories. Fig. 2 illustrates the processing of demolition concrete into recycled aggregates. After demolition, the concrete slabs were transported to a designated processing area, where they were crushed and screened to produce RCA of the required size fractions. Although residues of adhered mortar were present on the recycled aggregates, the parent concrete's high strength and durability contributed positively to the overall quality of the recycled material. Based on standard highway engineering practices in Pakistan and internationally, the concrete used for the pavement belongs to the C35/45 strength class.

### 2.2. Characterisation of aggregates

A comprehensive characterisation campaign was performed on both the fresh coarse aggregates (FCA) and the RCA prior to concrete production. The objective was to establish their physical, mechanical, and gradation properties, which directly affect concrete performance.



Fig. 2. Processing of demolition concrete waste for the production of recycled coarse aggregates in Pakistan: (a) collection of large concrete debris; (b) crushed material after primary breaking; (c) manual sorting before sieve processing.



Fig. 3. Sieve analysis of RCA: (a) loading the crushed material into the sieve stack; (b) manual agitation and intermediate separation of aggregate fractions; (c) collection of the sieved RCA retained on the target sieve size.

Sieve analysis was carried out following ASTM C136. Coarse aggregates were sieved through sizes ranging from 3 in to No. 4 (4.75 mm), and the resulting gradation curves and fineness modulus (FM) were obtained. Fine aggregates were analysed separately using sieves from No. 4 to No. 200 (75 μm). The FM values were used to evaluate the overall coarseness of the aggregates and their suitability for concrete mix proportioning (Fig. 3).

Specific gravity and water absorption were measured in accordance with AASHTO T85 and ASTM C127. These parameters are especially important for RCA because of the presence of adhered mortar and microcracks, which typically increase porosity and affect the concrete’s water demand. The unit weight of both FCA and RCA was determined using ASTM C29 procedures, providing insight into aggregate density and packing characteristics. Aggregate toughness was evaluated using the Aggregate Impact Value (AIV) test according to ASTM C131 and BS 812, while fineness modulus for coarse aggregates was further verified following ASTM C33. Table 2 summarizes all tests and associated standards.

### 2.3. Materials and preparation of recycled aggregates

All concrete mixes were produced using Ordinary Portland Cement (OPC) CEM I 42.5N, compliant with EN 197–1. Natural sand was sourced from the Lawrencepur region, and fresh coarse aggregates were obtained from the Margalla quarries. Potable tap water was used for mixing and curing.

The RCA was produced through the controlled processing of the GT Road demolition waste. After mechanical crushing, the material was

Table 2  
Aggregate characterisation tests and associated standards.

Test	Standard
Unit weight	ASTM C29–78
Water absorption	AASHTO T85; ASTM C127
Impact value	ASTM C131; BS 812
Specific gravity	AASHTO T85–10
Fineness modulus	ASTM C33

sieved according to ASTM C33 to isolate the target size fraction. All RCA was washed, oven-dried, and stored in labelled containers to ensure uniformity of moisture and grading. The nominal maximum aggregate size in the concrete mixes was 12.7 mm, while 19.5 mm fractions were used during sieve-based proportioning of the RCA.

### 2.4. Mix proportions and specimen configuration

Five concrete mixtures were prepared, corresponding to RCA replacement levels of 0%, 25%, 50%, 75%, and 100% by mass of coarse aggregates. All mixtures followed a 1:2:4 (cement:sand:coarse aggregate) proportion with a constant water–cement ratio of 0.50. Cement, sand, and water quantities were kept constant across all mixes, while FCA was progressively replaced by RCA. The mix proportions for each replacement level are summarised in Table 4. A total of 45 specimens were cast: 15 beams, 15 cubes, and 15 cylinders. For each RCA replacement level, three specimens of each type were produced. Table 3

**Table 3**  
Geometry, number of specimens, and associated standards.

S/N	Specimen	Geometry (mm)	Samples	Standard / Test
1	Beam	600 × 150 × 150	15	ASTM C78/C78M (Flexural)
2	Cube	150 × 150 × 150	15	ASTM C39 (Compression, 500 °C)
3	Cylinder	300 (H) × 150 (D)	15	ASTM C39 (Compression)

**Table 4**  
Mix design for beams, cubes and cylinders at different RCA replacement levels.

Mix Type	Beams	Cubes	Cyl.	Cement (kg)	Fresh CA (kg)	RCA (kg)
0% RCA	3	3	3	36	147	0
25% RCA	3	3	3	36	110.25	36.75
50% RCA	3	3	3	36	73.50	73.50
75% RCA	3	3	3	36	36.75	110.25
100% RCA	3	3	3	36	0	147

summarizes the geometry, quantity, and corresponding testing standard for each specimen.

All mixes were prepared in a mechanical drum mixer. Dry constituents were first homogenised, after which water was added gradually to ensure uniform hydration. The fresh concrete was placed into steel moulds for beams, cubes, and cylinders in three layers, each compacted by rodding 25 times. After finishing, moulds were kept in laboratory conditions for 24 hours, then demoulded and cured in water for 28 days. Before testing, specimens were dried and labelled.

Workability was assessed immediately after mixing using the slump test according to ASTM C143, see Fig. 4(a). Variations in slump values across mixes provided insight into the influence of RCA content on the flowability and consistency of fresh concrete.

It should be noted that each mixture was tested using three specimens, which provides an initial assessment of the RCA replacement effect but limits the statistical robustness of the results. In addition, although the RCA was washed, oven-dried, and stored under controlled laboratory conditions before mixing, no specific saturated-surface-dry moisture-conditioning procedure or water-absorption correction was applied; therefore, the high absorption capacity of RCA may have influenced the effective water-to-cement ratio and contributed to the observed variability. These aspects are acknowledged as limitations of the present experimental programme and should be addressed in future studies through larger sample sizes, controlled RCA moisture conditioning, and mix-water adjustment procedures.

### 2.5. Mechanical testing of hardened concrete

After curing, specimens underwent compression, flexural and splitting-tensile tests, as shown in Fig. 5.

Compressive strength tests on cubes and cylinders followed ASTM C39, enabling the determination of peak load, stress-strain response and energy absorption. Flexural performance was evaluated using three-point static loading of beams according to ASTM C138/C138M, with mid-span deflection monitored continuously. Crack initiation and propagation were documented throughout. Splitting tensile strength was measured following ASTM C496. Durability was assessed using the water absorption test per ACI guidelines, which provides insight into pore connectivity and permeability.

Non-destructive tests were conducted before destructive testing. Ultrasonic Pulse Velocity (UPV) measurements followed ASTM C597 to identify internal voids and microcracks. Schmidt rebound hammer testing, performed in line with ACI recommendations, provided surface hardness and an indirect estimate of compressive strength, see Fig. 6.

It should be noted that the present experimental programme was based on a single, traceable source of pavement-derived RCA; therefore, possible batch-to-batch variability associated with different demolition sources, parent concrete qualities, contamination levels, and processing conditions was not explicitly investigated. This aspect represents a limitation of the study and should be addressed in future research through multi-source and multi-batch experimental campaigns.

## 3. Experimental results

### 3.1. Characterisation of the aggregates

The physical characterisation of the aggregates is summarised in Fig. 7 and Table 5. The plot compares RCA aggregates and FCA ones for all key parameters relevant to concrete mix design, namely impact value, water absorption, specific gravity, unit weight, and fineness modulus. As shown, the RCA exhibits substantially higher water absorption and a lower specific gravity than the FCA, reflecting the presence of adhered mortar and internal microcracking typically associated with recycled aggregates. The RCA's higher impact value also indicates reduced toughness, consistent with its more heterogeneous composition.

Table 5 lists the numerical values of each measured property together with the corresponding ASTM and AASHTO standards used for testing. The results confirm that the RCA is lighter, more porous, and mechanically weaker than the FCA, as evidenced by its lower unit weight and higher absorption. Despite these variations, the fineness modulus of both aggregate types remains comparable, indicating similar grading characteristics after processing.



**Fig. 4.** Preparation and conditioning of concrete specimens: (a) measurement of slump to assess fresh concrete workability; (b) oven-drying of cubes and cylinders prior to testing; (c) 28-day water curing of beams and cylinders in a controlled tank.

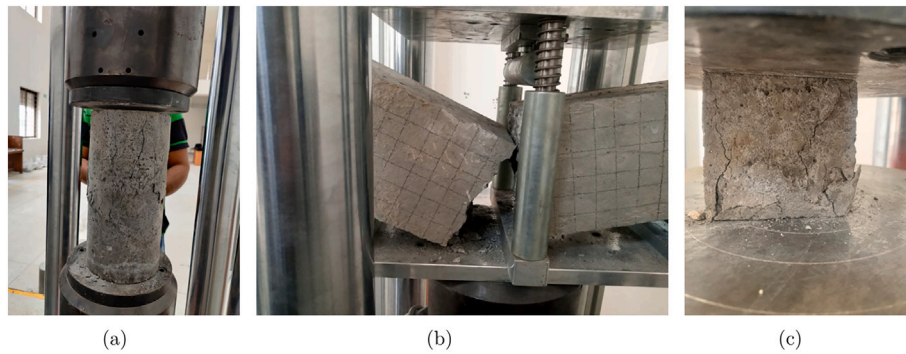


Fig. 5. Typical failure modes observed during mechanical testing: (a) compressive failure of a concrete cylinder under axial loading; (b) flexural failure of a beam during three-point bending; (c) compressive crushing of a cube specimen.

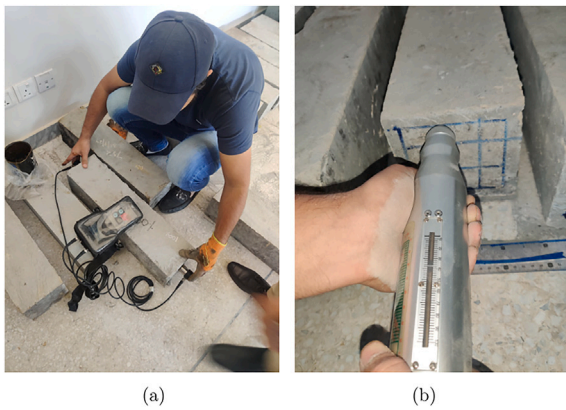


Fig. 6. Non-destructive assessment procedures: (a) transmission of ultrasonic pulses through concrete to evaluate homogeneity; (b) application of the Schmidt rebound hammer for surface hardness estimation.

The experimental results obtained in this study are consistent with the well-established behaviour of recycled coarse aggregates reported in the literature. The elevated water absorption of RCA (8.4%), which is more than eight times that of FCA, aligns with the ranges reported by

Silva et al. [57], who documented absorption values between 5% and 12% depending on the adhered mortar content and crushing conditions. The reduced specific gravity observed in this study (1.98 for RCA versus 2.42 for FCA) is similarly in agreement with findings by Katz [58] and Poon et al. [59], who attribute lower density to residual cement paste and microcracking. The increase in impact value (from 29.9% to 32.6%) is also consistent with earlier observations that RCA particles possess weaker mechanical integrity due to attached old mortar, as noted by Oikonomou [60]. Studies focusing on mechanical enhancement techniques, such as those by He et al. [61], further confirm that the inherent brittleness of RCA can affect performance unless mitigated by fibre reinforcement or surface treatment. Additionally, research on mortar removal techniques, such as the microwave-assisted chemical methods examined by Byeon and Ahn [62], supports the explanation that RCA quality strongly depends on the efficiency of adhered-mortar removal. Overall, the numerical differences measured in this study fall squarely within internationally reported ranges, reinforcing the validity and representativeness of the Pakistani RCA used in this work.

### 3.2. Nondestructive mechanical tests on concrete specimens

The in-situ mechanical response of the RCA concrete mixtures was initially assessed using the Schmidt rebound hammer, following the general principles of EN 12,504-2 and ACI recommendations. For each RCA replacement level (0%, 25%, 50%, 75%, and 100%), rebound numbers

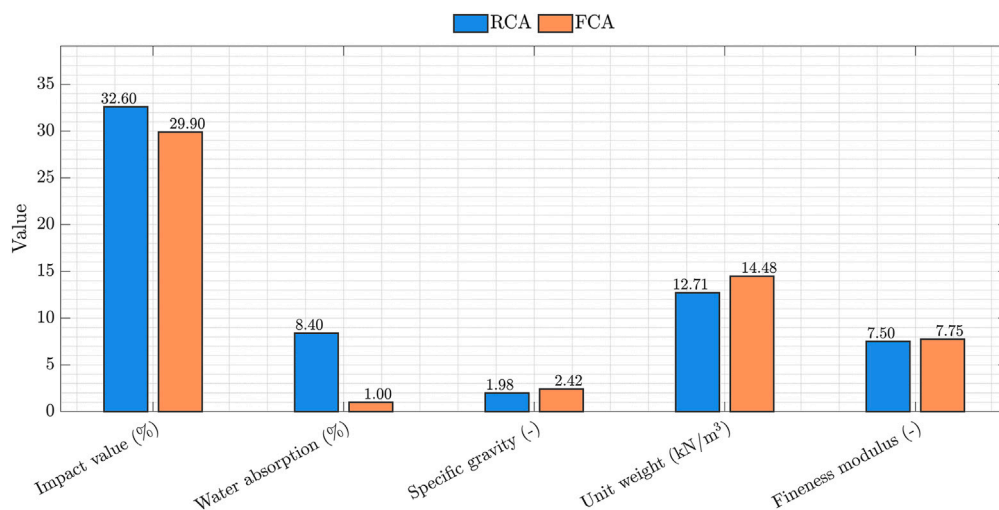


Fig. 7. Comparison of key physical properties of recycled coarse aggregates (RCA) and fresh coarse aggregates (FCA), including impact value, water absorption, specific gravity, unit weight, and fineness modulus. Error bars are omitted for clarity.

**Table 5**  
Physical properties of recycled coarse aggregates (RCA) and fresh coarse aggregates (FCA), along with the corresponding testing standards.

Sr. No.	Test	RCA	FCA	Standard
1	Impact value (%)	32.60	29.90	ASTM C131; BS 812
2	Water absorption (%)	8.40	1.00	AASHTO T85; ASTM C127
3	Specific gravity (-)	1.98	2.42	AASHTO T85-10
4	Unit weight (kg/m <sup>3</sup> )	1271.4	1447.7	ASTM C29-78
5	Fineness modulus (-)	7.50	7.75	ASTM C33

were recorded on beams, cubes, and cylinders at two orientations (0° and 90°) to account for surface anisotropy, operator positioning, and local heterogeneity. To convert rebound numbers into an estimated compressive strength, the empirical correlation

$$f_c = 0.035R^2 - 0.63R + 12.5, \tag{1}$$

This equation provides a quadratic mapping between the rebound index  $R$  and the expected compressive strength  $f_c$ , and its use is consistent with correlations reported in the literature for concrete in the 10–40 MPa range. Because rebound hammer readings are highly sensitive to surface texture, moisture content, carbonation depth, and the presence of adhered mortar on RCA, the estimated strength values should be viewed as comparative indicators rather than absolute strength predictions.

The error bars shown in Fig. 8 represent the standard deviation of 16 rebound measurements for each specimen type and RCA content,

capturing the statistical scatter inherent to the method. Higher RCA contents tended to exhibit both lower rebound indices and larger dispersion, reflecting the increased surface roughness, residual mortar, and microcracking typically associated with recycled aggregates. Conversely, the 0% and 25% RCA mixtures demonstrated more consistent readings and higher rebound-derived strength estimates, in line with their denser and more homogeneous microstructure.

The UPV measurements reported in Fig. 9 reveal the internal quality and stiffness of concrete incorporating RCA. At 0% RCA, beams exhibit a pulse velocity of 4069 m/s, followed by cubes (8380 m/s) and cylinders (2111 m/s), reflecting the influence of specimen geometry, transducer coupling, and travel path on wave propagation. As the RCA content increases, a consistent reduction in the velocity-to-length ratio ( $V/L$ ), commonly used as a proxy for dynamic elastic modulus in accordance with ASTM C597, is observed for all specimen geometries. This trend indicates progressive microstructural degradation associated with adhered mortar, higher porosity, and weaker ITZ typical of recycled aggregates.

For beam specimens,  $V/L$  decreases from 4.07 km/s at 0% RCA to 3.72 km/s at 100% RCA (an 8.7% reduction), while cylinders show a reduction from 4.22 km/s to 3.76 km/s (10.9%). Cube specimens exhibit a comparable sensitivity to RCA replacement, decreasing from 4.19 km/s to 3.71 km/s (11.4%). Overall, the UPV results confirm a progressive loss of material homogeneity and stiffness with increasing RCA content, consistent with the microstructural weakening trends widely reported for recycled-aggregate concrete.

Fig. 10 reports the WA results for beams, cubes, and cylinders across all RCA replacement levels. A clear and systematic increase in WA is

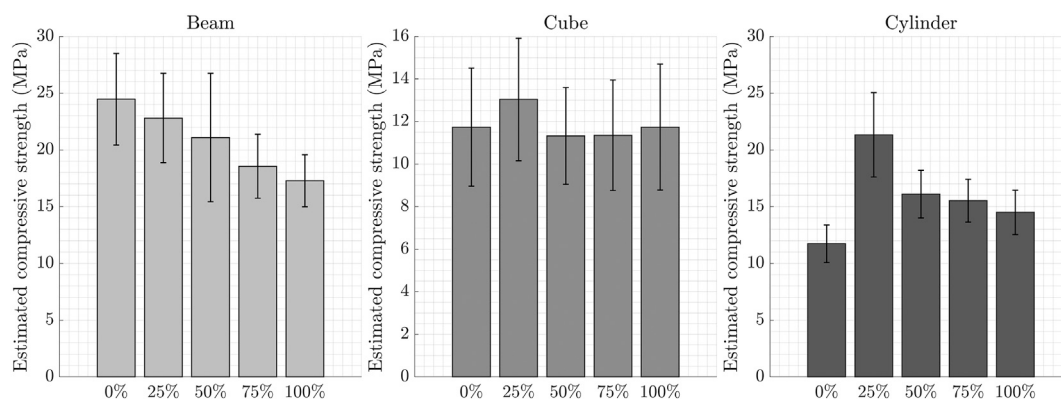


**Fig. 8.** Estimated compressive strength of concrete obtained from rebound hammer testing for beams, cubes, and cylinders produced with 0%, 25%, 50%, 75%, and 100% recycled coarse aggregate (RCA).

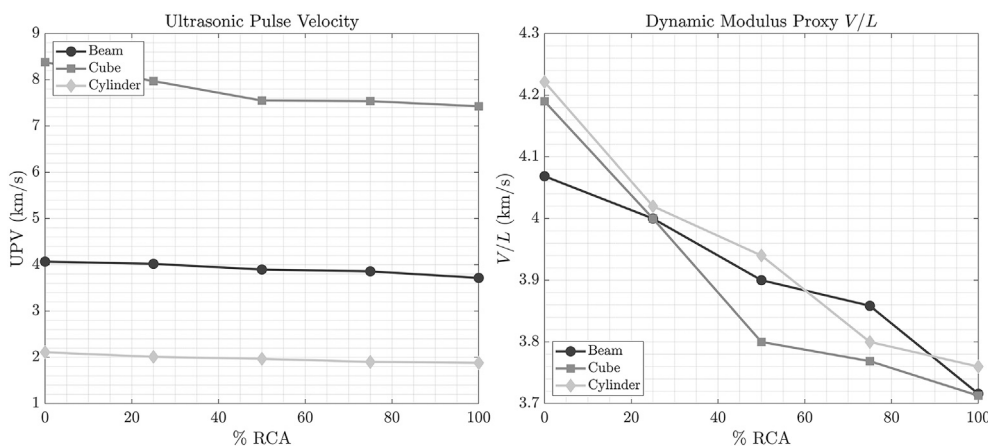


**Fig. 9.** Ultrasonic pulse velocity (UPV) and dynamic modulus proxy ( $V/L$ ) for beams, cubes, and cylinders incorporating 0%, 25%, 50%, 75%, and 100% recycled coarse aggregate (RCA).

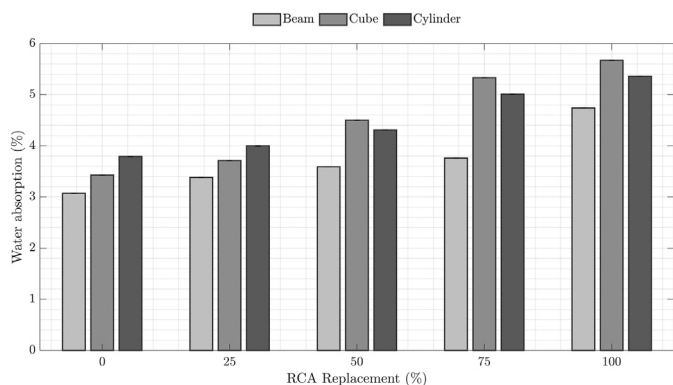


Fig. 10. Water absorption of beam, cube, and cylinder specimens produced with 0%, 25%, 50%, 75%, and 100% recycled coarse aggregate (RCA).

observed as the RCA content rises from 0% to 100%, irrespective of specimen geometry. This trend is consistent with the well-established behaviour of recycled aggregates, whose adhered mortar layer and higher microcrack density significantly increase open porosity and capillary suction compared with natural aggregates. For example, beam WA increases from 3.07% at 0% RCA to 4.74% at 100% RCA, while cylinders rise from 3.79% to 5.36% over the same range. Cubes show a similar progression, reaching 5.67% at full replacement.

The magnitude of the increase (approximately 45–60% relative to the control mix) aligns with values reported in the literature for unprocessed RCA derived from structural elements. The results confirm that the incorporation of RCA leads to higher permeability and water uptake, which may influence long-term durability properties such as shrinkage, freeze-thaw resistance, and chloride ingress. Nonetheless, the relatively moderate increase up to 50% replacement suggests that partial substitution remains feasible for non-aggressive exposure classes, provided appropriate mix design adjustments are adopted.

### 3.3. Destructive mechanical tests on concrete specimens

To evaluate the structural integrity and mechanical performance of concrete incorporating RCA, a series of destructive mechanical tests were conducted on beams, cylinders, and cubes. The RCA replacement levels ranged from 0% (control) to 100%, increasing in 25% increments. Each group was tested in triplicate to capture experimental variability. The primary tests performed included: (i) flexural testing on beams, (ii) compressive strength testing on both cylinders and cubes, and (iii) split tensile strength testing on cubes under

both ambient conditions and after exposure to elevated temperatures (500 °C).

Fig. 11 presents representative stress-strain curves for each specimen type and RCA replacement level. The beam responses (left panel) reveal a typical quasi-brittle behavior with limited strain capacity and a moderate strength decline as RCA content increases. Cubes (center) display more ductile profiles with strength peaks shifting as RCA. Cylinders (right) exhibit stiffer but more variable stress responses, with notable softening in samples with higher RCA content.

The compressive strength results are illustrated in Fig. 12, comparing the performance of cylindrical and cubic specimens. A general reduction in compressive strength is observed with increasing RCA content for both specimen types, attributed to weaker interfacial bonding and increased porosity in recycled aggregates. Error bars denote the standard deviation across the three replicates, indicating consistency in the test outcomes.

Fig. 13 summarizes three key mechanical indicators: (a) flexural strength of beams, (b) split tensile strength of cubes under ambient conditions, and (c) split tensile strength after thermal exposure. While flexural strength shows minor variation with RCA content, tensile strength at ambient conditions peaks at 50% RCA and then decreases. After exposure to 500 °C, tensile strength strongly increases in RCA mixes, indicating potential benefits of thermal conditioning for recycled mixes. These results emphasise that the mechanical performance of RCA-incorporated concrete remains competitive, especially in moderate substitution ratios, and even under elevated temperatures.

Table 6 summarizes the results of statistical analyses performed on the mechanical properties of concrete incorporating varying percentages of RCA, ranging from 0% to 100%. To assess whether RCA replacement significantly affects each property, one-way ANOVA tests were conducted across all groups.

The ANOVA results indicate that, for the tested dataset, none of the measured mechanical properties showed statistically significant differences among RCA replacement levels at the conventional  $\alpha = 0.05$  threshold. However, this result should not be interpreted as proof of equivalence among the mixtures, especially considering the limited number of specimens tested for each replacement level. Rather, it indicates that statistically significant differences were not detected within the variability and sample size of the present experimental programme.

Although clear trends were observed, such as the general decrease in compressive and flexural strength with increasing RCA content, the split tensile strength exhibited a non-monotonic response. In particular, the ambient-temperature split tensile strength showed an anomalous peak at 50% RCA, while the post-fire split tensile strength increased markedly at 75% RCA. These results deviate from the most commonly reported behaviour of recycled aggregate concrete, where tensile properties generally decrease with increasing RCA content. Therefore, the observed

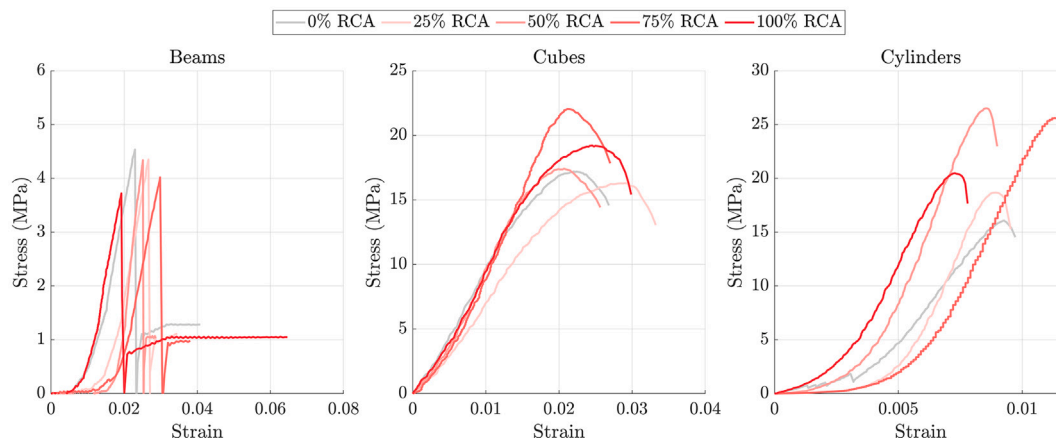


Fig. 11. Selected stress-strain responses of beams, cubes and cylinders incorporating 0–100% recycled coarse aggregate (RCA).

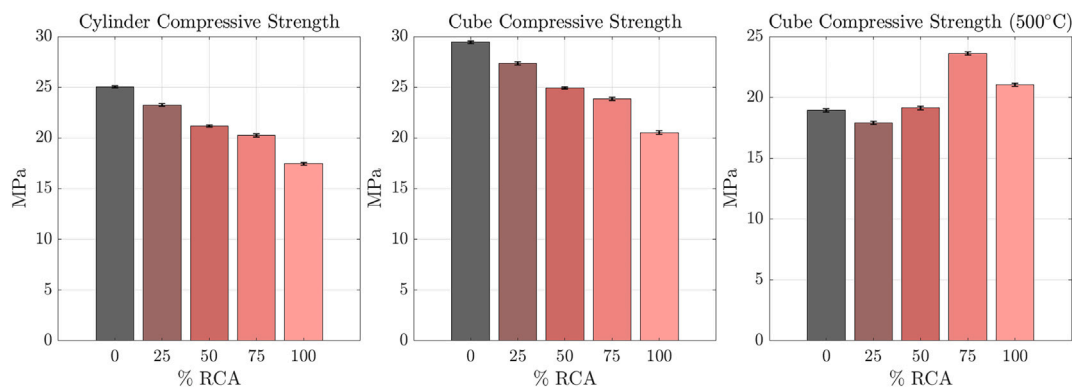


Fig. 12. Compressive strength comparison between cylindrical and cubic specimens incorporating recycled coarse aggregates (RCA) at 0–100% substitution rates. Results highlight a gradual reduction in strength, with error bars denoting experimental variability.

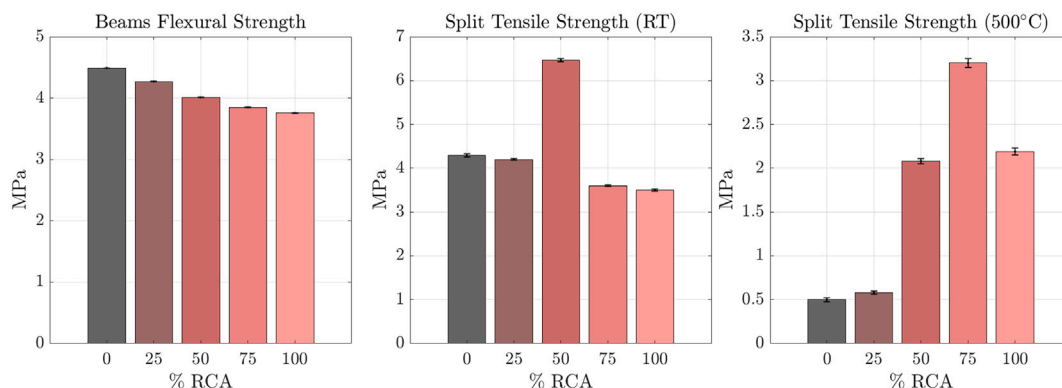


Fig. 13. Mechanical performance of recycled concrete at varying RCA replacement levels: (a) flexural strength of beams, (b) split tensile strength of cubes at ambient conditions (Room Temperature, RT), and (c) split tensile strength after exposure to 500 °C. Results include error bars showing the standard deviation across three replicates.

Table 6

Statistical summary of mechanical test results for different recycled concrete aggregate (RCA) replacement percentages. Values are reported as mean ± standard deviation (in MPa) based on three replicates for each group. Mechanical properties include: beam flexural strength, cylinder compressive strength, cube split tensile strength (at ambient and after 500 °C exposure), and cube compressive strength (at ambient and after 500 °C exposure).

RCA %	Beams	Cylinders	Split	Split @500 °C	Cubes	Cubes @500 °C
0	4.494 ± 0.020	25.020 ± 0.106	4.290 ± 0.036	0.500 ± 0.020	29.435 ± 0.125	18.940 ± 0.135
25	4.278 ± 0.012	23.240 ± 0.135	4.200 ± 0.017	0.580 ± 0.020	27.341 ± 0.159	17.920 ± 0.131
50	4.012 ± 0.032	21.173 ± 0.087	6.460 ± 0.036	2.080 ± 0.030	24.910 ± 0.103	19.140 ± 0.151
75	3.850 ± 0.042	20.260 ± 0.144	3.600 ± 0.017	3.200 ± 0.050	23.835 ± 0.170	23.620 ± 0.131
100	3.758 ± 0.056	17.450 ± 0.132	3.500 ± 0.020	2.190 ± 0.040	20.529 ± 0.156	21.040 ± 0.135
ANOVA p-val	–	0.6847	0.7267	0.4107	0.6847	0.4631

increases should be interpreted cautiously and should not be generalized without further validation.

A possible explanation for the peak at intermediate RCA replacement levels may be related to local particle-packing effects, internal curing promoted by the porous adhered mortar, or localized refinement of the cementitious matrix, as also suggested by the SEM observations at 50% RCA. Similarly, the improved residual split tensile response after exposure to 500 °C may be associated with the higher porosity of RCA mixtures, which could partially reduce thermally induced pore pressure and delay crack propagation under the specific testing conditions adopted. Nevertheless, these mechanisms remain hypotheses and require confirmation through additional specimens, different heating regimes, direct crack-pattern analysis, and fracture-based testing.

Accordingly, the anomalous tensile and post-fire trends are considered preliminary observations rather than definitive evidence of

improved performance. Further targeted investigation is required to verify whether these responses are repeatable and whether they are controlled by RCA content, aggregate source, moisture state, thermal exposure conditions, or specimen variability. These findings suggest that RCA incorporation produces measurable changes in mechanical behaviour, but the interpretation of non-monotonic tensile and post-fire responses should remain conservative.

#### 4. Discussion

While average trends reveal a progressive decline in mechanical strength with increasing RCA content, statistical analysis using one-way ANOVA showed that these reductions were not statistically significant at a 95% confidence level. This finding implies that even at 100% RCA replacement, concrete retains adequate performance for structural

applications—provided that design margins accommodate the increased variability. This trend is consistent with several previous investigations reporting that RCA incorporation usually causes gradual, rather than abrupt, mechanical degradation, especially when the recycled aggregate is obtained from relatively good-quality parent concrete and when replacement levels remain moderate [63,64]. At the aggregate level, the recycled material exhibited higher water absorption and lower specific gravity compared to natural aggregates, a trend widely reported in the literature [63,64]. The observed 8% water absorption in RCA, compared to just 1% in fresh aggregates, corresponds to the presence of adhered mortar and greater porosity, factors known to influence the mechanical integrity of concrete [65]. Similar increases in absorption capacity have been reported for recycled aggregates obtained from demolished concrete, where residual mortar and crushing-induced microcracks increase the volume of open pores and reduce aggregate density. Therefore, the physical properties measured in the present study fall within the expected range for untreated RCA and confirm the representativeness of the investigated Pakistani material source. This increased absorption capacity correlates with reduced compressive strength, particularly evident in both cube and cylinder tests, and supports earlier findings in the regional context [64].

The flexural strength of beam specimens demonstrated a modest increase at 50% RCA replacement, likely attributable to an optimized ITZ or particle packing effect [66]. This non-monotonic behavior has been documented in other hybrid or blended mixes, indicating that intermediate RCA levels may offer beneficial microstructural interactions under certain conditions. The present results therefore agree with studies showing that intermediate RCA contents may occasionally produce comparable or slightly improved tensile/flexural responses, provided that the recycled particles contribute to favourable packing, internal curing, or localized bridging effects within the cementitious matrix [66]. However, this beneficial effect should not be generalized to all RCA sources, as it remains strongly dependent on aggregate quality, adhered mortar content, and mixture proportioning.

Split tensile strength, especially after exposure to elevated temperature (500 °C), showed a pronounced decline. While RCA concrete exhibited a measurable post-fire strength, its degradation was more rapid than that of control specimens, aligning with previous thermal resistance studies [67]. This comparison with previous post-fire studies suggests that the old mortar attached to RCA and the pre-existing microcracks may intensify thermally induced damage. At the same time, the residual strength retained by the RCA mixtures confirms that recycled aggregate concrete can maintain a measurable load-bearing capacity after high-temperature exposure, in agreement with the general behaviour reported for RAC subjected to elevated temperatures [67].

Non-destructive test results provided further confirmation. Both rebound hammer values and UPV decreased with rising RCA content, reflecting internal microstructural looseness and increased pore connectivity. Nevertheless, values remained above structural acceptability thresholds, and dynamic modulus values derived from UPV never dropped below the 3.5 km/s cutoff often cited in structural assessments [68]. These findings demonstrate that RCA concretes preserve adequate stiffness and surface hardness for many applications. The observed decrease in UPV is consistent with previous studies in which RCA reduced wave velocity because of higher porosity, weaker ITZs, and increased microcrack density. The agreement between the destructive and non-destructive results strengthens the interpretation that the performance reduction is governed mainly by physical discontinuities introduced by adhered mortar rather than by an abrupt incompatibility between RCA and the new cement matrix [68].

Moreover, the statistical significance testing performed across all six mechanical properties confirmed that the variation between groups, while evident, was not statistically significant at the group level ( $p$ -values > 0.05). This reinforces conclusions from previous works suggesting that RCA concrete can be implemented in real-world structural

applications without reliability concerns, provided rigorous quality control is maintained [63,69]. Compared with the cited studies, the present work confirms the same general tendency: RCA increases variability and gradually reduces average performance, but does not necessarily prevent structural use when the recycled aggregate source is controlled and the replacement level is selected appropriately.

In the Pakistani context, these findings resonate with the conclusions of recent region-specific studies advocating for increased use of RCA in urban construction. They also support RCA as an effective waste management and sustainability strategy with marginal mechanical trade-offs [64,65]. The comparison with previous literature therefore indicates that the behaviour of the investigated pavement-derived Pakistani RCA is broadly consistent with international and regional evidence, while adding source-specific data for a local waste stream that has not been extensively documented.

## 5. Microstructural analysis

### 5.1. X-ray diffraction (XRD) analysis of RCA concrete

X-ray diffraction (XRD) analysis was performed to characterize the mineralogical composition of the tested concrete mixes. Fig. 14 shows XRD patterns of concrete samples. The diffractograms reveal the consistent presence of hydration-related phases such as portlandite ( $\text{Ca}(\text{OH})_2$ ), calcite ( $\text{CaCO}_3$ ), and quartz ( $\text{SiO}_2$ ), with changes in intensity distribution and background as RCA content increases, indicating higher amorphous C–S–H presence and residual crystalline phases.

Table 7 presents a comparative summary of the main XRD peaks identified across mixes with increasing RCA replacement. All the peaks are reported in Table 8. These results reveal important trends in the hydration and carbonation behaviour of the cementitious systems as RCA content increases.

The peak near  $18^\circ 2\theta$ , attributed to portlandite ( $\text{Ca}(\text{OH})_2$ ), is evident across all mixes, with maximum intensity observed at 50% RCA (27.4 counts), indicating enhanced hydration. This likely results from improved internal curing due to the water-absorptive nature of RCA. However, as RCA increases to 75% and 100%, the portlandite peak weakens (22.8 and 25.0 counts, respectively), suggesting reduced calcium hydroxide availability, either through dilution of clinker content or its progressive consumption via carbonation. The calcite peak, a product of carbonation, located at approximately  $29.5^\circ 2\theta$ , intensifies from 25% (52.7 counts) to 75% RCA (69.3 counts), highlighting a rising carbonation tendency with increasing RCA. Interestingly, the intensity decreases at 100% RCA (41.0 counts), implying a saturation of the carbonation process or a limit in portlandite availability for reaction. Quartz ( $\text{SiO}_2$ ) peaks, notably at  $26^\circ$  to  $36^\circ 2\theta$ , remain consistent throughout, as expected from the aggregate-rich composition of RCA. These peaks serve as internal mineralogical references and indicate the inert contribution of quartz phases. The broader presence of smaller peaks, especially in the 75% RCA sample, points to an increasingly heterogeneous phase composition. This may reflect localized recrystallization, phase segregation, or microstructural refinement. Although the total peak intensity remains balanced, the structural complexity increases with higher RCA content.

The 50% RCA mix exhibits optimal hydration activity, while 75% RCA reflects the highest carbonation potential. At 100% RCA, a stabilizing effect is observed, possibly due to the dilution of reactive components. These findings suggest that moderate RCA incorporation (e.g., 50%) may achieve a balance between hydration and durability, whereas higher levels promote carbonation but could compromise long-term structural development.

### 5.2. Scanning electron microscopy (SEM) analysis

SEM was employed to investigate the microstructural evolution of concrete incorporating increasing levels of RCA. SEM observations reveal distinct morphological differences between NA and RCA. Natural aggregates exhibit sharp angular geometry with dense and relatively

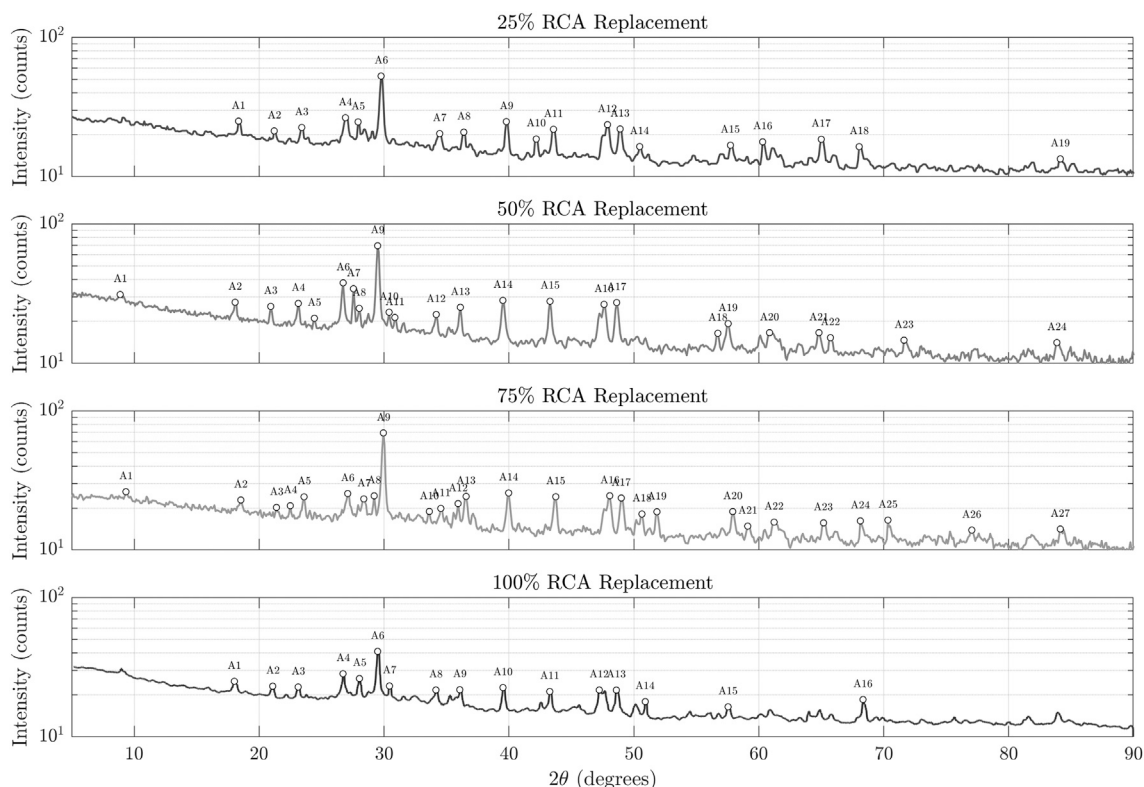


Fig. 14. X-ray diffraction (XRD) patterns of concrete samples incorporating 25%, 50%, 75%, and 100% recycled coarse aggregate (RCA) replacement.

Table 7

Key XRD peaks identified across RCA replacement levels and associated mineral phases.

2θ (°)	Phase	Assignment	25%	50%	75%	100%
18.0–18.5	Portlandite (Ca(OH) <sub>2</sub> )	Hydration product	25.0	27.4	22.8	25.0
21.1–21.4	C-S-H / Quartz	Background / Silicate base	21.3	25.6	20.2	23.1
23.1–23.6	Ettringite / C-S-H	Sulfate phase	22.5	26.9	24.1	22.8
26.7–27.1	Quartz (SiO <sub>2</sub> )	Major quartz peak	26.5	37.7	25.4	28.4
29.4–29.9	Calcite (CaCO <sub>3</sub> )	Carbonation peak	52.7	69.6	69.3	41.0
34.0–36.5	Quartz / Minor hydration	Crystalline silica variants	20.3–24.8	25.2–28.3	18.9–24.2	21.7–23.2
43.2–43.7	Quartz / Calcite	Overlap zone	21.9	27.8	24.1	21.1
47.2–48.9	Quartz	Mid-intensity crystalline peak	23.6	26.5	24.5	21.7
57.5–58.0	Quartz (SiO <sub>2</sub> )	Weak phase	16.8	19.3	18.9	16.4
68.0–68.3	Quartz (SiO <sub>2</sub> )	Weak high-angle phase	16.4	16.2	16.2	18.5

smooth surfaces, indicative of low intrinsic porosity and strong mineral integrity. In contrast, RCA particles display rounded and irregular morphologies, highly porous surfaces, microcracks, and extensive adhered old cement mortar, reflecting their origin from crushed hardened concrete. Particular attention was given to the ITZ, since this region controls stress transfer between the aggregate and the surrounding cement paste. The SEM images allow a qualitative comparison between the relatively compact NA–paste interface and the more heterogeneous RCA–paste interface. In the case of natural aggregates, the ITZ appears denser and more continuous, with fewer visible pores and microcracks. Conversely, the RCA–paste interface is characterized by a rougher aggregate surface, residual old mortar, local microcracking, and a thicker porous transition zone. This difference reflects the coexistence of the old ITZ inherited from the parent concrete and the newly formed ITZ between the RCA and the fresh cement paste.

At 25% RCA replacement (Fig. 15), the hydration matrix is primarily composed of amorphous calcium–silicate–hydrate (C–S–H), providing a relatively compact microstructure. However, localized weak ITZ regions are already visible around RCA particles, where residual old mortar promotes higher porosity and microcracking. Bright,

irregular clusters observed near RCA surfaces correspond to calcium-rich hydration products, including portlandite (Ca(OH)<sub>2</sub>) and secondary calcite (CaCO<sub>3</sub>) formed through carbonation of residual paste, consistent with XRD results. The comparison between Figs. 15(a) and (d) highlights the different quality of the aggregate–paste interfaces. Around the natural aggregate, the matrix appears relatively compact and continuous, suggesting a stronger and more homogeneous NA–paste bond. In contrast, the RCA–paste interface shows a visibly thickened ITZ with localized porosity and discontinuities. This confirms that even at low RCA replacement, the recycled particles introduce additional interfacial heterogeneity compared with natural aggregates.

At the intermediate replacement level of 50% RCA (Fig. 16), the microstructure exhibits a notable presence of acicular, needle-like crystalline features, typically 500–1000 nm in length. These features are consistent with ettringite and related calcium sulfoaluminate hydration products formed during early and secondary hydration stages. Their formation is promoted by the availability of sulfate ions and calcium hydroxide released from the adhered mortar on RCA particles. At this replacement level, the fine distribution of acicular phases within capillary pores appears to partially bridge adjacent hydration

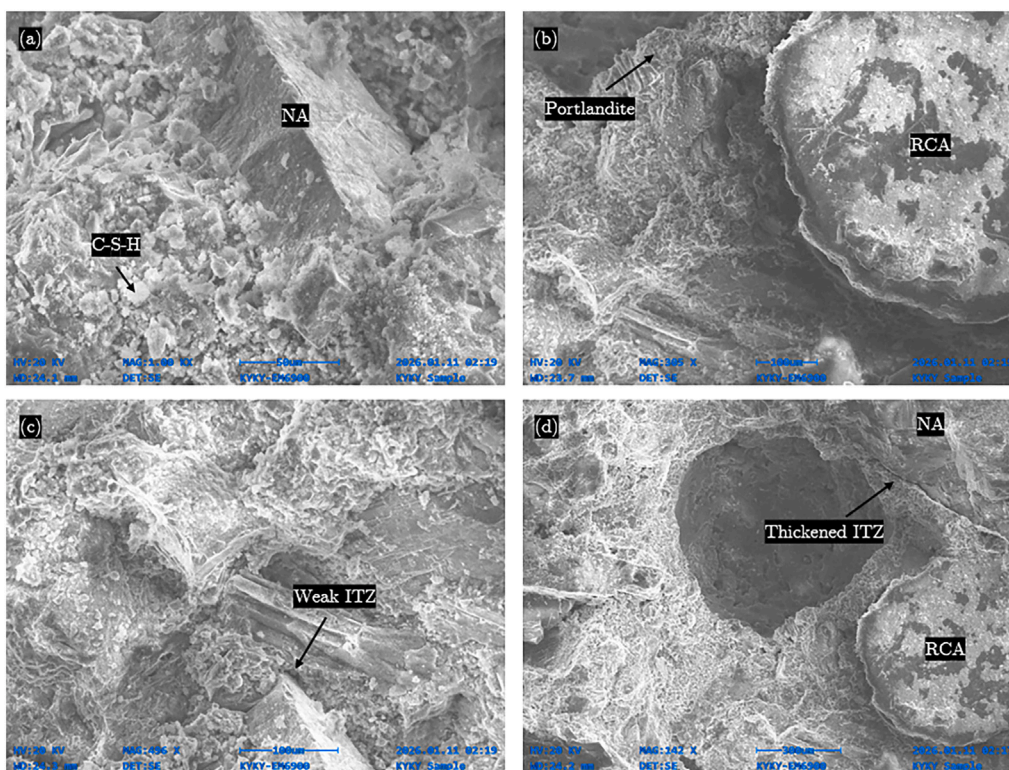


**Fig. 15.** SEM micrographs of concrete with 25% RCA replacement: (a) dense natural aggregate (NA) embedded in a hydration matrix dominated by C–S–H gel; (b) RCA particle with adhered old mortar and portlandite-rich regions; (c) weakened interfacial transition zone (ITZ) characterized by microcracking and porous hydration products; (d) thickened ITZ at the RCA–paste interface highlighting increased heterogeneity compared to natural aggregates.

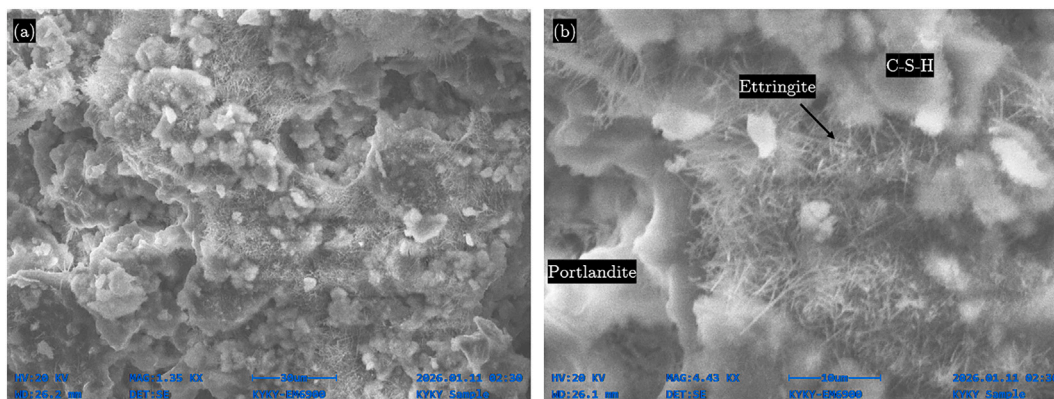


**Fig. 16.** SEM micrograph of concrete with 50% RCA replacement showing needle-like crystalline features consistent with ettringite and related calcium sulfoaluminate hydration products.

products, contributing to local matrix refinement without inducing extensive cracking. This balanced microstructural condition supports the experimentally observed mechanical behavior, where moderate RCA incorporation does not result in statistically significant degradation of structural performance. From an ITZ perspective, the 50% RCA mixture suggests a transitional condition between the compact NA-dominated matrix and the more porous RCA-dominated microstructure. The presence of needle-like hydration products within pores and interfacial regions may partially densify the matrix and reduce the negative effect of the RCA–paste interface. This observation helps explain why intermediate RCA contents can maintain acceptable mechanical performance despite the presence of recycled aggregate surfaces.

At 75% RCA replacement (Fig. 17), the microstructure becomes increasingly heterogeneous, with a higher concentration of macro- and capillary pores embedded within the C–S–H-rich matrix. The increased porosity is primarily associated with the cumulative effect of adhered old mortar and pre-existing microcracks within RCA particles. Locally brighter, plate-like regions attributed to portlandite-rich phases are also observed, in agreement with XRD analyses. These features indicate incomplete densification of the hydration matrix and help explain the gradual reduction in mechanical performance observed at higher RCA contents. Compared with the lower replacement levels, the ITZ at 75% RCA is less localized and becomes part of a more continuous heterogeneous network. The larger number of RCA particles increases

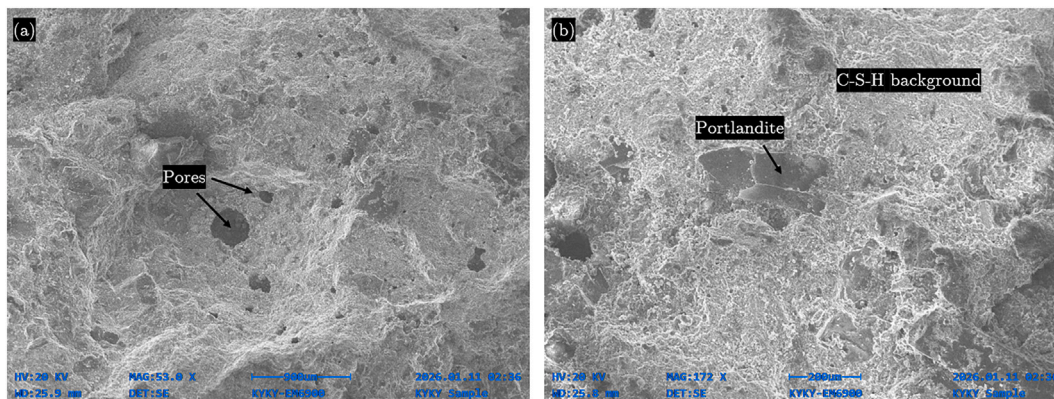


Fig. 17. SEM micrograph of concrete with 75% RCA replacement showing a heterogeneous microstructure with increased macro- and capillary pore content.

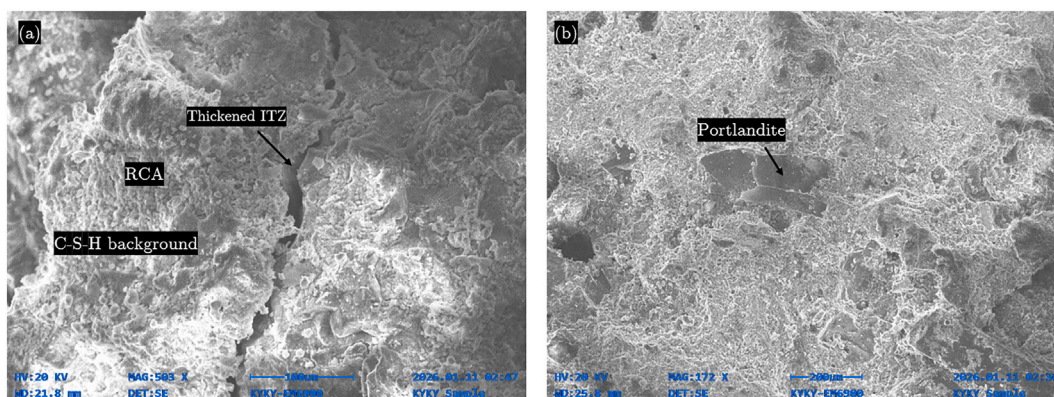


Fig. 18. SEM micrographs of concrete incorporating 100% RCA replacement highlighting a rough RCA surface, a thickened interfacial transition zone (ITZ), and calcium-rich hydration products.

the probability of overlapping weak zones, including old mortar regions, old ITZs, and newly formed RCA–paste interfaces. As a result, the microstructure contains more preferential paths for crack initiation and moisture transport, which is consistent with the increase in water absorption and the reduction in mechanical strength observed experimentally.

Fig. 18 illustrates the microstructural features of concrete incorporating 100% RCA. RCA particles are characterized by rough, highly porous surfaces with extensive adhered old mortar, embedded within a C–S–H-rich hydration matrix. A markedly thickened ITZ is observed at the RCA–paste interface, reflecting the coexistence of the old ITZ from the parent concrete and the newly formed ITZ in the recycled system. This widened and more porous interfacial zone represents a critical weak region, contributing to increased heterogeneity, elevated permeability, and reduced mechanical efficiency. Plate-like, portlandite-rich regions are frequently observed, consistent with XRD findings. Overall, the SEM observations provide microstructural evidence explaining the increased porosity and the gradual reduction in mechanical performance at full RCA replacement. In contrast to the NA–paste interface observed at low RCA content, the 100% RCA mixture is governed almost entirely by RCA–paste interfaces. The ITZ is therefore not limited to isolated regions but becomes a dominant microstructural feature. The presence of rough RCA surfaces, adhered old mortar, microvoids, and calcium-rich hydration products indicates a more complex and weaker interfacial system than that of natural aggregate concrete.

Fig. 19 presents the energy-dispersive X-ray spectroscopy (EDS) spectra of concrete specimens incorporating increasing recycled coarse aggregate (RCA) contents, together with the quantitatively extracted

integrated areas of the characteristic  $K\alpha$  emission bands of C, O, Al, and Si. The EDS results provide semi-quantitative insight into the evolution of elemental composition associated with the progressive replacement of natural aggregates with recycled material.

At low RCA content (25–50%), the integrated areas of the major elemental bands remain relatively limited, reflecting a matrix still dominated by natural aggregates and newly formed hydration products. In particular, the moderate carbon and oxygen signals are consistent with a limited presence of adhered old mortar and carbonation products. Correspondingly, the aluminium and silicon bands exhibit lower intensities, indicating a reduced contribution from aluminosilicate-rich phases typically associated with recycled concrete fines.

A pronounced increase in all elemental band areas is observed at higher RCA replacement levels (75–100%). The substantial rise in the C– $K\alpha$  and O– $K\alpha$  integrated areas highlights the increasing influence of carbonated phases and hydrated cement products, in agreement with SEM observations showing extensive C–S–H gel and portlandite-rich regions surrounding RCA particles. Simultaneously, the marked growth of the Al– $K\alpha$  and Si– $K\alpha$  bands indicates a higher contribution of aluminosilicate phases, attributable to the presence of adhered old mortar and residual cementitious material on recycled aggregates.

Notably, the strongest integrated areas are recorded at 100% RCA replacement, particularly for the Si– $K\alpha$  and Al– $K\alpha$  bands, confirming the dominance of silica- and alumina-bearing phases within the microstructure. This compositional shift is consistent with XRD results showing persistent quartz and calcite peaks and with SEM evidence of a thickened and more heterogeneous interfacial transition zone (ITZ). While these compositional changes reflect increased heterogeneity and

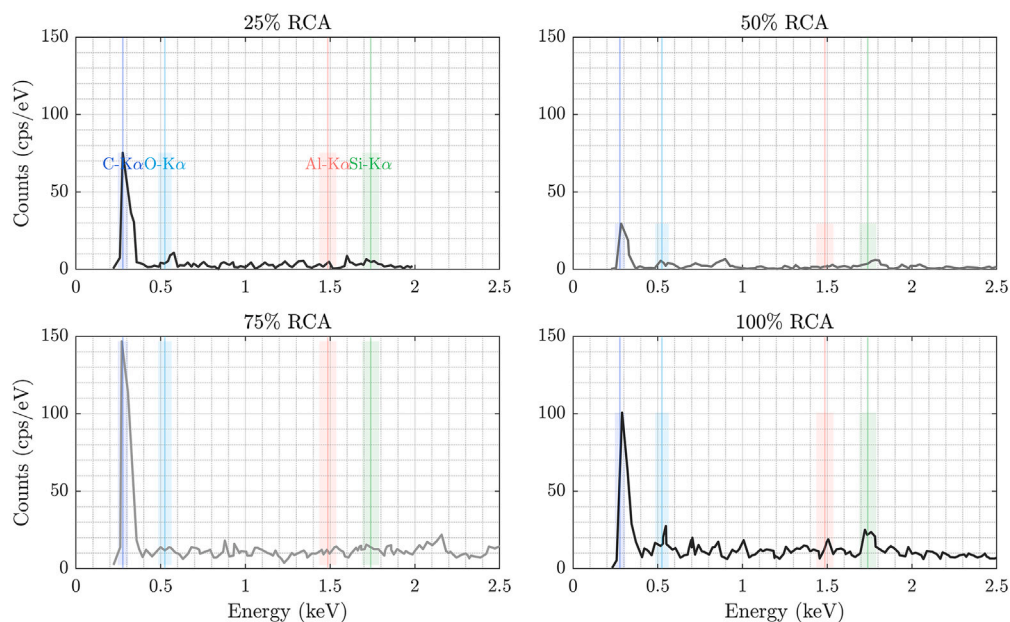


**Fig. 19.** Energy-dispersive X-ray spectroscopy (EDS) spectra of concrete incorporating 25%, 50%, 75%, and 100% recycled coarse aggregate (RCA). Vertical shaded bands indicate the characteristic  $K\alpha$  emission ranges of carbon (C), oxygen (O), aluminium (Al), and silicon (Si).

porosity, they do not translate into statistically significant mechanical degradation, as demonstrated by the mechanical testing results. Overall, the EDS analysis corroborates the microstructural interpretation that RCA incorporation primarily modifies the phase distribution and elemental composition of the matrix rather than inducing abrupt material incompatibilities. The EDS results also support the comparative ITZ interpretation obtained from SEM. The increase in C, O, Al, and Si signals at higher RCA contents is consistent with the greater amount of adhered old mortar and aluminosilicate-rich residual cementitious phases surrounding RCA particles. This confirms that the RCA–paste interface differs chemically and morphologically from the NA–paste interface, which is comparatively denser and less affected by residual hydrated mortar.

### 5.3. Discussion

XRD results show that RAC contains the same primary hydration and carbonation phases as conventional concrete, namely calcium–silicate–hydrate (C–S–H), portlandite ( $\text{Ca}(\text{OH})_2$ ), calcite ( $\text{CaCO}_3$ ), and quartz ( $\text{SiO}_2$ ). Variations in peak intensities with increasing RCA content are consistent with literature findings and reflect the combined effects of internal curing, adhered old mortar, and enhanced carbonation susceptibility [70–72]. Moderate RCA contents tend to increase portlandite availability due to internal water release from the porous recycled aggregates, promoting continued hydration. At higher replacement levels, however, portlandite is progressively consumed by carbonation, leading to an increase in calcite peaks and a relative depletion of  $\text{Ca}(\text{OH})_2$ , a trend widely reported for RCA systems [70].

The persistent quartz reflections across all replacement levels confirm that the inert mineral fraction of the aggregates remains largely unchanged, while the diffuse amorphous hump between  $20\text{--}30^\circ 2\theta$  indicates sustained formation of C–S–H gel. This demonstrates that the cement hydration mechanism is not fundamentally disrupted by RCA incorporation but rather modulated by dilution and internal curing effects [71]. Secondary hydration products, particularly ettringite, are inferred from both XRD peak features and SEM observations of acicular crystals, consistent with sulfate availability from adhered old mortar [72].

SEM analysis reveals that the most significant microstructural modification induced by RCA is the development of a more heterogeneous and porous ITZ. RCA particles exhibit rough, irregular surfaces with attached old mortar, microcracks, and higher intrinsic porosity compared to natural aggregates, in agreement with previous investigations [73–75]. Unlike conventional concrete, RCA contains multiple ITZs: an old ITZ within the recycled aggregate, a new ITZ between old mortar and fresh paste, and, in some cases, direct stone–paste interfaces. These overlapping ITZs increase the volume fraction of weak zones and promote crack initiation and propagation [75].

At moderate replacement levels (25–50%), SEM images show that these microstructural weaknesses remain localized. Needle-like hydration products, with lengths on the order of 500–1000 nm, were observed at 50% RCA and are consistent with ettringite morphology. Such features can locally refine the microstructure by filling pores and bridging hydration products, provided their growth remains limited [76]. This explains why moderate RCA contents often exhibit negligible or statistically insignificant reductions in mechanical performance, as also reported by Limbachiya et al. [70].

At higher replacement levels (75–100%), SEM observations reveal an increase in capillary and macroporosity, wider and more porous ITZs, and extensive microcracking. These features are directly linked to the higher volume of adhered mortar and the reduced quality of the aggregate–paste bond [73,77,78]. The resulting microstructure is less uniform and mechanically less efficient, explaining the gradual strength reductions typically reported for high-RCA concretes.

EDS analysis supports these observations by showing systematic increases in the integrated areas of C, O, Al, and Si bands with increasing RCA content. The enhanced carbon and oxygen signals reflect increased carbonation and hydrated paste content, while higher aluminium and silicon intensities indicate a greater contribution of aluminosilicate-rich phases from the adhered mortar [73].

## 6. Conclusions

This study assessed the feasibility of incorporating recycled coarse aggregates (RCA), derived from locally sourced construction and

demolition waste in Pakistan, as partial or total substitutes for natural coarse aggregates in concrete. The experimental programme combined aggregate characterization, destructive mechanical testing, non-destructive evaluation, residual assessment after exposure to 500 °C, and microstructural analyses using XRD, SEM, and EDS for RCA replacement levels ranging from 0% to 100%. The study specifically focused on pavement-derived RCA obtained from a traceable local waste stream, and the conclusions should therefore be interpreted within the limits of this material source, mixture design, curing regime, and laboratory testing programme.

The physical characterization confirmed that the investigated RCA had higher water absorption and lower specific gravity than natural coarse aggregate. These differences were mainly associated with adhered old mortar, crushing-induced microcracks, and higher intrinsic porosity. Although these characteristics did not prevent the production of concrete with acceptable mechanical properties, they increased the sensitivity of the mixtures to RCA content and indicate the need for careful control of aggregate moisture condition, grading, and mix proportioning when RCA is used in structural concrete.

Mechanical testing showed a progressive reduction in compressive and flexural strength as the RCA replacement level increased. Concrete mixtures containing up to 50% RCA achieved 28-day compressive strengths close to or above 25 MPa, indicating their potential suitability for structural-grade applications under the investigated conditions. At higher replacement levels, particularly 75% and 100% RCA, the concrete still retained measurable load-bearing capacity, but the reduction in average strength, the increase in porosity, and the greater microstructural heterogeneity suggest that these mixtures should not be generally recommended for structural use without additional mix optimization, durability verification, and source-specific quality control. Therefore, the results support the use of RCA most confidently at moderate replacement levels, especially up to 50%, rather than an unrestricted use at full replacement.

The non-destructive test results were consistent with the destructive mechanical trends. Rebound hammer and UPV measurements generally decreased with increasing RCA content, indicating a gradual loss of surface hardness, internal compactness, and dynamic stiffness. These results confirm that NDT methods can provide useful complementary information for evaluating RCA concrete quality, but they should be interpreted together with mechanical tests because RCA-induced surface roughness, porosity, and moisture sensitivity may influence the measured response.

Thermal exposure at 500 °C showed that RCA concrete retained residual mechanical capacity after heating. However, the post-fire results should be considered preliminary because only one temperature level and one exposure condition were investigated. While the presence of adhered mortar and internal porosity did not lead to an abrupt loss of residual performance in the tested specimens, further work is required to evaluate different temperature levels, heating durations, cooling regimes, and residual durability before drawing general conclusions on the fire performance of RCA concrete.

Microstructural investigations showed that RCA incorporation did not fundamentally alter the main hydration products of concrete. XRD confirmed the presence of typical cementitious phases, including C–S–H-related features, portlandite, calcite, and quartz. SEM observations revealed that the main microstructural effect of increasing RCA content was the progressive development of thicker, more porous, and more heterogeneous interfacial transition zones. EDS analyses further indicated increasing contributions from carbonated and aluminosilicate-rich phases with increasing RCA content, consistent with the larger amount of adhered old mortar. These findings suggest that the mechanical response of the investigated RCA concrete was governed primarily by physical and interfacial effects rather than by deleterious chemical incompatibility between RCA and the new cement matrix.

The results indicate that locally sourced pavement-derived RCA can be used as a sustainable partial replacement for natural coarse aggregate

in concrete in Pakistan, particularly at replacement levels up to 50% under the investigated conditions. The study provides source-specific evidence supporting the valorisation of concrete pavement waste, but it does not eliminate the need for additional validation before broad structural implementation.

**CRedit authorship contribution statement**

**Nisar Ali Khan:** Writing – review & editing, Validation, Supervision, Resources, Methodology, Investigation, Funding acquisition, Formal analysis, Data curation, Conceptualization. **Angelo Aloisio:** Writing – review & editing, Writing – original draft, Visualization, Validation, Supervision, Methodology, Investigation, Formal analysis, Data curation, Conceptualization. **Rafia Younas:** Validation, Supervision, Methodology, Investigation, Formal analysis. **Flavio Stochino:** Validation, Investigation. **Giorgio Monti:** Validation, Supervision, Conceptualization.

**Availability of data and material**

All data, models, or codes supporting this study’s findings are available from the corresponding author upon request.

**Declaration of competing interest**

The authors declare that they have no known competing financial interests or personal relationships that could have appeared to influence the work reported in this paper.

**Appendix A**

**Table 8**  
Main peaks of the XRD analyses.

% Replacement	Label	2θ	Intensity	% Replacement	Label	2θ	Intensity
25	A1	18.35	25.03	75	A1	9.34	26.20
25	A2	21.21	21.29	75	A2	18.54	22.83
25	A3	23.41	22.54	75	A3	21.39	20.19
25	A4	26.91	26.49	75	A4	22.49	20.76
25	A5	27.92	24.72	75	A5	23.60	24.08
25	A6	29.76	52.66	75	A6	27.09	25.41
25	A7	34.45	20.37	75	A7	28.38	23.26
25	A8	36.39	20.86	75	A8	29.21	24.46
25	A9	39.79	24.84	75	A9	29.95	69.33
25	A10	42.18	18.64	75	A10	33.63	18.89
25	A11	43.56	21.87	75	A11	34.55	19.87
25	A12	47.89	23.62	75	A12	35.93	21.52
25	A13	48.90	21.98	75	A13	36.57	24.24
25	A14	50.46	16.45	75	A14	39.97	25.68
25	A15	57.73	16.81	75	A15	43.75	24.11
25	A16	60.31	17.78	75	A16	48.07	24.49
25	A17	65.00	18.56	75	A17	48.99	23.60
25	A18	68.03	16.42	75	A18	50.65	18.12
25	A19	84.13	13.42	75	A19	51.84	18.79
50	A1	8.88	31.12	75	A20	57.91	18.86
50	A2	18.08	27.39	75	A21	59.11	14.81
50	A3	20.93	25.58	75	A22	61.23	15.83
50	A4	23.14	26.87	75	A23	65.18	15.64
50	A5	24.43	21.04	75	A24	68.13	16.16
50	A6	26.73	37.74	75	A25	70.33	16.38
50	A7	27.55	34.25	75	A26	77.05	13.87
50	A8	28.01	24.77	75	A27	84.13	14.12
50	A9	29.49	69.61	100	A1	18.02	25.01
50	A10	30.41	23.25	100	A2	21.09	23.08
50	A11	30.87	21.31	100	A3	23.13	22.77
50	A12	34.18	22.39	100	A4	26.72	28.38
50	A13	36.11	25.21	100	A5	28.03	26.19

(continued on next page)

Table 8 (continued)

% Replacement	Label	2θ	Intensity	% Replacement	Label	2θ	Intensity
50	A14	39.51	28.25	100	A6	29.49	41.00
50	A15	43.29	27.84	100	A7	30.43	23.16
50	A16	47.61	26.45	100	A8	34.15	21.69
50	A17	48.62	27.25	100	A9	36.06	21.78
50	A18	56.72	16.41	100	A10	39.52	22.56
50	A19	57.55	19.25	100	A11	43.27	21.14
50	A20	60.86	16.57	100	A12	47.23	21.68
50	A21	64.81	16.57	100	A13	48.60	21.65
50	A22	65.73	15.27	100	A14	50.91	17.89
50	A23	71.62	14.65	100	A15	57.54	16.42
50	A24	83.86	14.07	100	A16	68.34	18.52

References

[1] Silva R, de Brito J, Dhir R. Properties and composition of recycled aggregates from construction and demolition waste suitable for concrete production. *Constr Build Mater* 2014;65:201–17.

[2] Jian S-M, Wu B. Compressive behavior of compound concrete containing demolished concrete lumps and recycled aggregate concrete. *Constr Build Mater* 2021;272:121624.

[3] Deng DA. A fast-developing market: an insight into China's construction and demolition waste recycling industry. *Jan* 2023. <https://www.investni.com/media-centre/features/insight-chinas-construction-and-demolition-waste-recycling-industry>.

[4] Chen LZ, Chen CY. Construction and demolition waste management: a review. *J Clean Prod* 2021;287:120594.

[5] IIPS. Construction waste and its impact on the environment; 2019 <https://iips.com.pk/construction-waste-and-its-impact-on-the-environment/> [accessed: 13 December 2025].

[6] Zheng L, Wu H, Zhang H, Duan H, Wang J, Jiang W, Song Q, et al. Characterizing the generation and flows of construction and demolition waste in China. *Constr Build Mater* 2017;136:405–13. <https://doi.org/10.1016/j.conbuildmat.2017.01.055>

[7] Villoria-Sáez P, Osmani M. A diagnosis of construction and demolition waste generation and recovery practice in the European Union. *J Clean Prod* 2019;241:118400. <https://doi.org/10.1016/j.jclepro.2019.118400>

[8] Aslam MS, Huang B, Cui L. Review of construction and demolition waste management in China and USA. *J Environ Manag* 2020;264:110445. <https://doi.org/10.1016/j.jenvman.2020.110445>

[9] Ministry of Housing and Urban Affairs (India). Government released comprehensive guidelines for effective disposal of C&D waste; 2024. <https://pib.gov.in/PressReleasePage.aspx?PRID=2007086>.

[10] Nunes KRA, Mahler CF, Valle R, Neves C. Comparison of construction and demolition waste management between Brazil, European Union and USA. *Waste Management & Research* 2020;38(4):415–22. <https://doi.org/10.1177/0734242X20916510>

[11] Ministry of Land, Infrastructure and transport, Japan, construction recycling promotion plan (annual report on construction recycling). In: Proceedings of the CIB international conference on sustainable building; 2002.

[12] Korea Ministry of Environment. Annual waste generation report 2020. in korean 2021.

[13] UK Department for Environment. Food & rural affairs, UK statistics on waste (sept 2022 edition); 2022. <https://www.gov.uk/government/statistics/uk-waste-data>.

[14] Jahan I, Zhang G, Bhuiyan M, Navaratnam S, Shi L. Experts' perceptions of the management and minimisation of waste in the Australian construction industry. *Sustainability* 2022;14(18):11319. <https://doi.org/10.3390/su141811319>

[15] Canadian Council of Ministers of the Environment. Guide for identifying, evaluating and selecting policies for influencing construction, renovation and demolition waste management; 2019. <https://ccme.ca/en/res/crdguidance-secured.pdf>.

[16] Naeem Z. Beyond the plastic debate. *The News International* (Pakistan); 16 Aug 2025. URL:<https://www.thenews.com.pk/latest/1336167-beyond-the-plastic-debate>.

[17] Limbachiya MC, Meddah MS, Seneviratne O. Use of recycled aggregate in concrete: a review. *J Sustain Cem-Based Mater* 2012;1(2):134–45.

[18] Hansen TC. Recycling of concrete. *J Mater Civ Eng* 1992;4(3):249–64.

[19] Katz A. Properties of concrete made with recycled aggregate. *J Mater Civ Eng* 2003;15(5):531–8.

[20] Topu Z. Effects of recycled aggregate on the mechanical properties of concrete. *J Mater Civ Eng* 2013;25(10):1431–8.

[21] Ali MS. Usps Pakistan contact from project procurement international; 2020. <http://projectpi.pk/>.

[22] Ali T, Qureshi MZ, Onyelowe KC, Althaqafi E, Deifalla A, Ahmed H, Ajwad A. Optimizing recycled aggregate concrete performance with chemically and mechanically activated fly ash in combination with coconut fiber. *Sci Rep* 2025;15(1):9346.

[23] Junior GA, Leite JC, Mendez G. D. P., Haddad AN, Silva JA, da Costa BB. A review of the characteristics of recycled aggregates and the mechanical properties of concrete produced by replacing natural coarse aggregates with recycled ones-fostering resilient and sustainable infrastructures. *Infrastructures* 2025;10(8):213.

[24] Tam VWY, Soomro M, Evangelista ACJ. A review of recycled aggregate in concrete applications (2000–2017). *Constr Build Mater* 2018;172:272–92.

[25] Gholampour A, Gandomi AH, Ozbakkaloglu T. New formulations for mechanical properties of recycled aggregate concrete using gene expression programming. *Constr Build Mater* 2017;130:122–45.

[26] Pacheco J, de Brito J, Chastre C, Evangelista L. Experimental investigation on the variability of the main mechanical properties of concrete produced with coarse recycled concrete aggregates. *Constr Build Mater* 2019;201:110–20.

[27] Singh R, Nayak D, Pandey A, Kumar R, Kumar V. Effects of recycled fine aggregates on properties of concrete containing natural or recycled coarse aggregates: a comparative study. *J Build Eng* 2022;45:103442.

[28] Xuan D, Zhan B, Poon CS. Durability of recycled aggregate concrete prepared with carbonated recycled concrete aggregates. *Cem Concr Compos* 2017;84:214–21.

[29] Wang B, Yan L, Fu Q, Kasal B. A comprehensive review on recycled aggregate and recycled aggregate concrete, resources. *Conservation and Recycling* 2021;171:105565.

[30] Huda SB, Alam MS. Mechanical and freeze-thaw durability properties of recycled aggregate concrete made with recycled coarse aggregate. *J Mater Civ Eng* 2015;27(7):04015003.

[31] Peng Q, Wang L, Lu Q. Influence of recycled coarse aggregate replacement percentage on fatigue performance of recycled aggregate concrete. *Constr Build Mater* 2018;169:347–53.

[32] Bian J, Zhang W, Shen Z, Li S, Chen Z. Analysis and optimization of mechanical properties of recycled concrete based on aggregate characteristics. *Sci Eng Compos Mater* 2021;28(4):516–27.

[33] Brandes MR, Kurama YC. Behavior of shear-critical prestressed concrete beams with recycled concrete aggregates under ultimate loads. *Eng Struct* 2018;165:237–46.

[34] Kou SC, Poon CS. Enhancing the durability properties of concrete prepared with coarse recycled aggregate. *Constr Build Mater* 2012;35:69–76.

[35] Sasanipour H, Aslani F. Durability properties evaluation of self-compacting concrete prepared with waste fine and coarse recycled concrete aggregates. *Constr Build Mater* 2020;234:117336.

[36] Makul N. Cost-benefit analysis of the production of ready-mixed high-performance concrete made with recycled concrete aggregate: a case study in Thailand. *Heliyon* 2020;6(6).

[37] Silva S, Evangelista L, de Brito J. Durability and shrinkage performance of concrete made with coarse multi-recycled concrete aggregates. *Constr Build Mater* 2021;272:121645.

[38] Akbarnezhad A, Ong KCG, Tam CT, Zhang MH. Effects of the parent concrete properties and crushing procedure on the properties of coarse recycled concrete aggregates. *J Mater Civ Eng* 2013;25(12):1795–802.

[39] Nedeljkovic M, Visser J, Šavija B, Valcke S, Schlangen E. Use of fine recycled concrete aggregates in concrete: a critical review. *J Build Eng* 2021;38:102196.

[40] Abed MA, Tayeh BA, Bakar BA, Nemes R. Two-year non-destructive evaluation of eco-efficient concrete at ambient temperature and after freeze-thaw cycles. *Sustainability* 2021;13(19):10605.

[41] Russo N, Lollini F. Effect of carbonated recycled coarse aggregates on the mechanical and durability properties of concrete. *J Build Eng* 2022;51:104290.

[42] Le H, Bui Q. Recycled aggregate concretes—a state-of-the-art from the microstructure to the structural performance. *Constr Build Mater* 2020;257:119522.

[43] Duan Z, Han N, Singh A, Xiao J. Multi-scale investigation on concrete prepared with recycled aggregates from different parent concrete. *J Renew Mater* 2020;8(14):1375–90.

[44] Rangel CS, Filho RDT, Amario M, Pepe M, de Castro Polisseni G, Puente de Andrade G. Generalized quality control parameter for heterogeneous recycled concrete aggregates: a pilot scale case study. *J Clean Prod* 2019;208:589–601.

[45] Ali T, Qureshi MZ, Onyelowe KC, Althaqafi E, Deifalla A, Ahmed H, Ajwad A. Optimizing recycled aggregate concrete performance with chemically and mechanically activated fly ash in combination with coconut fiber. *Sci Rep* 2025;15:9346.

[46] Panghal H, Kumar A. Enhancing concrete performance: surface modification of recycled coarse aggregates for sustainable construction. *Constr Build Mater* 2024;411:134432. <https://doi.org/10.1016/j.conbuildmat.2023.134432>

[47] Panghal H, Kumar A. Enhancing concrete durability and strength: an innovative approach integrating abrasion and cement slurry treatment for recycled coarse aggregates. *Struct Concr* 2025;26(2):1455–76. <https://doi.org/10.1002/suco.202400387>

[48] Panghal H, Kumar A. Enhancing concrete performance with treated recycled aggregates: a comparative study of coating, chemical, and abrasion treatments. *Iran J Sci Technol Trans Civ Eng* 2025;49:1173–91. <https://doi.org/10.1007/s40996-024-01633-0>

[49] Marinkovic S, Radonjanin V, Malešev M, Ignjatović I. Comparative environmental assessment of natural and recycled aggregate concrete. *Waste Manag* 2010;30(11):2255–64.

[50] Kleijer AL, Lasvaux S, Citherlet S, Viviani M. Product-specific life cycle assessment of ready mix concrete: comparison between a recycled and an ordinary concrete, resources. *Conservation and Recycling* 2017;122:210–8.

[51] Xing W, Tam VWY, Le KN, Hao JL, Wang J. Life cycle assessment of recycled aggregate concrete on its environmental impacts: a critical review. *Constr Build Mater* 2022;317:125950.

[52] Katerusha D. Barriers to the use of recycled concrete from the perspective of executing companies and possible solution approaches—case study Germany and Switzerland. *Resour Policy* 2021;73:102212.

[53] Xiao J, Li J, Zhang C. Mechanical properties of recycled aggregate concrete under uniaxial loading. *Cem Concr Res* 2005;35(6):1187–94.

- [54] Xu J, Chen Z-P, Ozbakkaloglu T, Demartino C. A critical assessment of the compressive behavior of reinforced recycled aggregate concrete columns. *Eng Struct* 2018;161:161–75.
- [55] Tayeh BA, Saffar DMA, Alousf R. The utilization of recycled aggregate in high performance concrete: a review. *J Mater Res Technol* 2020;9(5):8469–81.
- [56] Younis A, Ebead U, Judd S. Life cycle cost analysis of structural concrete using seawater, recycled concrete aggregate, and GFRP reinforcement. *Constr Build Mater* 2018;175:152–60.
- [57] Silva RV, de Brito J, Dhir RK. Properties and composition of recycled aggregates from construction and demolition waste suitable for concrete production. *Constr Build Mater* 2014;65:201–17.
- [58] Katz A. Properties of concrete made with recycled aggregate from partially hydrated old concrete. *Cem Concr Res* 2003;33(5):703–11.
- [59] Poon CS, Shui ZH, Lam L. Effect of microstructure of itz on compressive strength of concrete prepared with recycled aggregates. *Constr Build Mater* 2004;18:461–8. <https://doi.org/10.1016/j.conbuildmat.2004.03.005>
- [60] Oikonomou ND. Recycled concrete aggregates. *Cem Concr Compos* 2005;27(2):315–8.
- [61] He W, Kong X, Fu Y, Zhou C, Zheng Z. Experimental investigation on the mechanical properties and microstructure of hybrid fiber reinforced recycled aggregate concrete. *Constr Build Mater* 2020;261:120488.
- [62] Byeon M-W, Ahn J-H. Removal of adhered mortar from recycled aggregate using microwave irradiation and a mixed hcl–h<sub>2</sub>O<sub>2</sub> solution. In: Proceedings of the Korean society of waste management conference; 2015. p. 23, in Korean; title translated by authors.
- [63] Alamri M, Ali T, Ahmed H, Qureshi MZ, Elmagarhe A, Khan MA, Ajwad A, Mahmood MS. Enhancing the engineering characteristics of sustainable recycled aggregate concrete using fly ash, metakaolin and silica fume. *Heliyon* 2024;10(7):e029014. <https://doi.org/10.1016/j.heliyon.2024.e29014>
- [64] Islam ZU, Farooq S, Shoaib M, Ishfaq M, Ahmad T, Ahmad H. Evaluating the mechanical properties of recycled aggregate concrete with variable coarse and fine aggregate replacements. *Discov Civ Eng* 2025;2(1):1–21. <https://doi.org/10.1007/s44290-025-00336-3>
- [65] Hameed R, Al-Soudani M, Amlil ASA, Ali H, Shahzad S, Hameed A. Impact of parent concrete strength of recycled aggregates on the mechanical performance of rac bricks. *Revista de la Construcción* 2025;24(2):505–32. <https://doi.org/10.7764/RDLC.24.2.505>
- [66] Momeni E, Omidinasab F, Dalvand A, Goodarzimehr V, Eskandari A. Flexural strength of concrete beams made of recycled aggregates: an experimental and soft computing-based study. *Sustainability* 2022;14(18):11769. <https://doi.org/10.3390/su141811769>
- [67] Varona FB, Baeza-Brotons F, Tenza-Abril AJ, Baeza FJ, Bañón L. Residual compressive strength of recycled aggregate concretes after high temperature exposure. *Materials* 2020;13(8):1981. <https://doi.org/10.3390/ma13081981>
- [68] Espinosa AB, Revilla-Cuesta V, Skaf M, Faleschini F, Ortega-López V. Utility of ultrasonic pulse velocity for estimating the overall mechanical behavior of recycled aggregate self-compacting concrete. *Appl Sci* 2023;13(2):874. <https://doi.org/10.3390/app13020874>
- [69] Al-Naghi AAA, Ali T, Inam I, Qureshi MZ, Kahla NB, Ghazouani N. An innovative approach to enhancing the strength and durability of recycled aggregate concrete through fly ash-silica fume coating and rice husk ash supplementation. *Sci Rep* 2025;15(1):32780. <https://doi.org/10.1038/s41598-025-18138-z>
- [70] Limbachiya M, Marrocchino E, Koulouris A. Chemical–mineralogical characterization of coarse recycled concrete aggregate. *Waste Manag* 2007;27(2):201–8.
- [71] Aghililoft M, Ramezani-pour AM, Bamshad O, Hajimohammadi A. Long-term performance of recycled aggregate concrete incorporating natural zeolite. *Struct Concr* 2025;26(6):7816–46.
- [72] Mozumder RS, Hoque MM, Taki MZH, Bhowmik MC, Sheikh P, Saha N. Durability assessment methods of co<sub>2</sub>-treated recycled concrete aggregate for transportation infrastructure. *Discov Civ Eng* 2025;2(1):213.
- [73] Alim MI, Mohiuddin KA. Micro-characterization of recycled concrete aggregate. *J Eng Sci* 2023;14(2):145–55.
- [74] Forero JA, Brito J. D. , Evangelista L, Pereira C. Improvement of the quality of recycled concrete aggregate subjected to chemical treatments: a review. *Materials* 2022;15(8):2740.
- [75] Tamayo P, Pacheco J, Thomas C, de Brito J, Rico J. Mechanical and durability properties of concrete with coarse recycled aggregate produced with electric arc furnace slag concrete. *Appl Sci* 2019;10(1):216.
- [76] Wu J, Ding Y, Xu P, Zhang M, Guo M, Guo S. Effects of carbonated recycled concrete aggregates on the mechanical properties of concrete and the micro-properties of the interfacial transition zone. *Ceramics-Silikáty* 2022;66(1):113–27.
- [77] Liu J, Ma K, Shen J, Zhu J, Long G, Xie Y, Liu B. Influence of recycled concrete aggregate enhancement methods on the change of microstructure of itzs in recycled aggregate concrete. *Constr Build Mater* 2023;371:130772.
- [78] Memon SA, Bekzhanova Z, Murzakarimova A. A review of improvement of interfacial transition zone and adherent mortar in recycled concrete aggregate. *Buildings* 2022;12(10):1600.